UCRL-JC-124617 Version date: February 27, 1997

On the effective viscoelastic moduli of two-phase media. II. Rigorous bounds on the complex shear modulus in three dimensions

Graeme W. Milton
Department of Mathematics
University of Utah
Salt Lake City, Utah 84112

and

James G. Berryman[*]
Lawrence Livermore National Laboratory
P. O. Box 808 L-202
Livermore, CA 94551-9900

[*]Address for correspondence.

Abstract

Cherkaev-Gibiansky and Hashin-Shtrikman variational principles are utilized in order to obtain rigorous bounds on the shear modulus of two-phase viscoelastic composites in three dimensions. The simplest class of bounding regions is composed of circles in the complex plane containing four points related to the viscoelastic moduli of the constituents. By taking the intersection of all such circles, we obtain tight bounds on the complex shear modulus. A compact algorithm for computing this region of intersection is formulated and tested. Several examples of bounding sets computed using the method are presented. When the phases have equal and real Poisson's ratio, the bounding set reduces to a simple lens-shaped region in the complex shear modulus plane. A mixture of two viscous fluids and a suspension of solid particles in a viscous fluid provide physical motivations for two other examples of bounds that have been computed. In the important limiting case when all the constituent moduli are real, the new shear modulus bounds are shown to reduce precisely to the well-known Hashin-Shtrikman-Walpole bounds.

1 Introduction

This paper is a continuation of the paper by Gibiansky & Milton (1993) on rigorous bounds for the moduli of viscoelastic two-phase composites. Part I described how both the translation method (Murat & Tartar 1985; Lurie & Cherkaev 1986; Milton 1990) and Hashin-Shtrikman-Walpole-type variational principles (Hashin & Shtrikman 1963; Walpole 1966) could be used to construct lens-shaped regions in the complex plane bounding the complex bulk modulus of such viscoelastic composites. The present paper (Part II) extends the Hashin-Shtrikman-type results to obtain similar lens-shaped regions in the complex plane bounding the complex shear modulus of such composites.

The early literature on this subject is very sparse, containing only a handful of papers (Hashin 1965; 1970; Christensen 1969; Roscoe 1969; 1972). The major development that has allowed recent progress to be made is the discovery by Cherkaev & Gibiansky (1994) of rigorous variational principles for problems with complex moduli [also see Milton (1990) and Fannjiang & Papanicolaou (1994)]. Since the publication of Part I, there has been renewed interest in the topic of bounds on viscoelastic constants with papers appearing by Gibiansky & Lakes (1993; 1997), Gibiansky, Lakes, & Milton (1993), Li & Weng (1994), and Brinson & Lin (1997), among others. For example, Li & Weng (1994) have checked the compatibility of the Mori-Tanaka approximation scheme with the complex bulk modulus bounds for various inclusion shapes and have found that these estimates always lie on or within the bounds. Gibiansky & Lakes (1993) obtained bounds on the complex bulk modulus assuming that the volume fractions are unknown. Their approach can also be used to generate volume-fraction independent bounds on complex shear moduli from the results we obtain in the present paper. Gibiansky & Lakes (1997) also derived bounds on the complex shear modulus of two-dimensional composites assuming a single scalar restriction on the moduli that is valid if, in particular, the two phases have real and equal Poisson's ratios. Other recent and related advances include work by Li & Weng (1997) and by Gibiansky & Torquato (1997).

The problem of obtaining bounds on the shear modulus for viscoelastic composites shares some significant similarities with the problem for bounds on the bulk modulus, but there are also some significant differences as well. We show how the Hashin-Shtrikman variational principle can be utilized to obtain bounds on the shear modulus. This part of the analysis has considerable overlap with that presented in Part I. The translation method, although it can certainly be applied to the problem of obtaining shear modulus bounds in three dimensions, has more degrees of freedom than the Hashin-Shtrikman-type method and, therefore, has even more constants to be determined. For this reason, the translation method has not been explored at this point in sufficient detail to warrant its inclusion in the present paper. A preliminary investigation of the translation method for the two-dimensional complex shear modulus has been initiated by Gibiansky & Lakes (1997) and also by Gibiansky & Milton (1997).

As was pointed out in Part I, the complex bulk-modulus bounds have a very similar structure to the bounds on the complex conductivity of isotropic two-phase composites, with fixed volume fractions of the phases, obtained by one of the present authors (Milton 1980; 1981) and independently by Bergman (1980; 1982) using a different method. That method is based on the analytic properties of the effective conductivity as a function of the two-components conductivities. Of more immediate relevance to the problem of bounding the viscoelastic shear-modulus is the two-dimensional complex dielectric problem, which is equivalent to the problem of bounding the complex axial shear modulus under torsion (or antiplane loading) of a viscoelastic composite with microgeometry independent of x_3. This equivalence is called the longitudinal shearing-transverse conduction analogy by Hashin (1983). For two-phase composites with transverse isotropy, optimal bounds were obtained by Milton (1980; 1981): these are attained by doubly coated cylinder assemblages.

To describe our results, let κ_1, μ_1, κ_2, μ_2, and κ_*, μ_* denote the complex bulk and shear moduli of the first and second constituent materials and the composite, respectively. Let

$$\kappa_* = \left[\sum_{i=1}^{2} \frac{f_i}{\kappa_i + y_\kappa}\right]^{-1} - y_\kappa \tag{1}$$

and

$$\mu_* = \left[\sum_{i=1}^{2} \frac{f_i}{\mu_i + y_\mu}\right]^{-1} - y_\mu, \tag{2}$$

where the volume fractions of the constitutents are f_1, f_2, respectively, and y_κ and y_μ are the Y-transforms [see Milton (1990) and references therein] of the bulk and shear moduli, respectively. The notation we will use distinguishes the the single point μ_* representing the actual effective shear modulus from the μ-plane, and similarly the single point y_μ related to μ_* through (2) is distinguished from the Y_μ-plane. Part I found bounds on y_κ, while the present paper will show that bounds on y_μ are determined by the following constraints: The desired point y_μ lies inside any circle in the complex Y_μ-plane that excludes the origin while containing the four points

$$\gamma(c)\mu_j \quad \text{and} \quad \gamma(c)\kappa_j/c \quad \text{for} \quad j = 1, 2, \tag{3}$$

where

$$\gamma(c) \equiv \frac{8 + 9c}{6(2 + c)}, \tag{4}$$

with c being a real number in the range $0 \le c \le \infty$. The desired bounds on y_μ are found by varying c over its range of allowed values and considering the intersection of all such constraining circles. Figure 1 shows a schematic of a single step in the process. Bounds on μ_* are then found by transforming back to the complex μ-plane using (2). Alternatively, (2) may be inverted to give y_μ in terms of μ_* [see (32)]. Comparisons to experimental data may therefore be performed either in the μ-plane or in the Y_μ-plane.

Section 2 presents the full development of the Hashin-Shtrikman variational method for bounds on viscoelastic constants. The results are then specialized to bounds on the shear modulus and a general result is obtained showing that these bounds take the form of circles in either the complex Y_μ-plane or the complex μ-plane. Further restrictions are then placed on the parameters determining the bounds. It is shown, for one four-dimensional subset of the six-dimensional parameter set, that the bounds on y_μ and the constraints on κ_1,κ_2,μ_1,μ_2 (for a given parameter choice) can all be expressed in terms of matrix inequalities of the same basic form. Section 3 then shows how these matrix inequalities can be given a geometric interpretation. Specifically, the circular bounding region containing y_μ may be characterized by the fact that it must contain the four points listed in Equation (3), but not the origin. Section 4 considers what is probably the simplest type of example possible for the shear modulus bounds, one in which the bounding region is determined by arcs of only two circles. Section 5 demonstrates that the bounds obtained here reduce precisely to the Hashin-Shtrikman-Walpole bounds when all the constituent moduli are real. Section 6 develops a Legendre transform approach to obtain a concise description of the general algorithm for constructing convex hulls, and then provides a worked example. Section 7 summarizes the general algorithm for shear modulus bounds. Section 8 provides further examples of the results obtained from the algorithm. Section 9 concludes with a general discussion and summary of our results. The Appendix contains some details needed in the derivations of Section 2.

The reader who is interested in the results but not in the theory may skip directly to Section 7 for the algorithm summary. We also recommend that any codes developed from the present work to compute bounding regions for the shear modulus be based on the formulas found in Section 7, as these are straightforward to code and have relatively few special cases that must be considered.

2 Theoretical development of the bounds

2.1 Formulating the Hashin-Shtrikman variational principle

Using the notation of Part I, we will treat the problem of the complex constitutive relation for viscoelasticity in the presence of harmonic oscillations using

$$\sigma = \mathcal{C}\varepsilon, \tag{1}$$

where σ and ε are complex stress and strain fields and $\mathcal{C}$ is a complex fourth rank symmetric tensor, all of which depend on the frequency of oscillation of the applied field. We assume without loss of generality that σ, ε, and $\mathcal{C}$ are periodic. This constitutive relation, written in terms of complex quantities, may be reformulated in terms of purely real quantities by considering

$$\mathbf{j} = \mathbf{D}\mathbf{e}, \tag{2}$$

where, in terms of the real and imaginary parts of σ and ε,

$$\mathbf{j} = \begin{pmatrix} \varepsilon'' \\ \sigma'' \end{pmatrix}, \qquad \mathbf{e} = \begin{pmatrix} -\sigma' \\ \varepsilon' \end{pmatrix}, \tag{3}$$

with the two ε's satisfying the differential constraint of a strain field $[\varepsilon = \frac{1}{2}(\nabla u + (\nabla u)^T)]$ and the two σ's satisfying the differential constraint of a stress field $(\nabla \cdot \sigma = 0)$, and

$$\mathbf{D} = \begin{pmatrix} (\mathcal{C}'')^{-1} & (\mathcal{C}'')^{-1}\mathcal{C}' \\ \mathcal{C}'(\mathcal{C}'')^{-1} & \mathcal{C}'' + \mathcal{C}'(\mathcal{C}'')^{-1}\mathcal{C}' \end{pmatrix}. \tag{4}$$

The Hashin-Shtrikman-type variational principle described previously in Part I (Gibiansky & Milton 1993) shows that the following inequality holds for the present problem:

$$\mathbf{e}_* \cdot (\mathbf{D_0} - \mathbf{D}_*)\mathbf{e}_* - 2\langle \mathbf{e}_* \cdot \mathbf{p}(\mathbf{x})\rangle \leq -\left\langle \mathbf{p}(\mathbf{x}) \cdot (\mathbf{D}_0 - \mathbf{D}(\mathbf{x}))^{-1}\mathbf{p}(\mathbf{x})\right\rangle + \langle \mathbf{p}(\mathbf{x}) \cdot \mathbf{e}_0(\mathbf{x})\rangle, \tag{5}$$

where the various terms in this inequality have the following meanings: The $\mathbf{D}$'s are all extended 12×12 tensors in viscoelasticity, with $\mathbf{D}(\mathbf{x})$ containing the spatially varying material constants and having the form of (4), $\mathbf{D}_*$ being the desired effective tensor and also having the form of (4), and $\mathbf{D}_0$ being a reference tensor, which is not necessarily of the form (4). The extended (12 component) vectors appearing in (5) are the applied field $\mathbf{e}_*$, $\mathbf{p}(\mathbf{x})$ an arbitrary polarization field, and $\mathbf{e}_0(\mathbf{x})$ which is obtained from an auxilliary problem to be described.

The auxilliary problem is completely analogous to the one that generates electric fields from an arbitrary polarization field. It has the form

$$\mathbf{p}(\mathbf{x}) - \mathbf{D}_0\mathbf{e}_0(\mathbf{x}) = \mathbf{j}_0(\mathbf{x}), \qquad \langle \mathbf{e}_0(\mathbf{x})\rangle = 0, \tag{6}$$

with

$$\mathbf{j}_0 = \begin{pmatrix} \varepsilon_0'' \\ \sigma_0'' \end{pmatrix}, \qquad \mathbf{e}_0 = \begin{pmatrix} -\sigma_0' \\ \varepsilon_0' \end{pmatrix}, \tag{7}$$

where again the two ε_0's satisfy the differential constraint of a strain field $[\varepsilon_0 = \frac{1}{2}(\nabla u_0 + (\nabla u_0)^T)]$ and the two σ_0's satisfy the differential constraint of a stress field $(\nabla \cdot \sigma_0 = 0)$.

The (largely arbitrary) reference tensor appearing in both (5) and (6) is taken to be of the form

$$\mathbf{D}_0 = \begin{pmatrix} \mathcal{A}(\alpha_{11}/d, \beta_{11}/2) & \mathcal{A}(\alpha_{12}, \beta_{12}) \\ \mathcal{A}(\alpha_{12}, \beta_{12}) & \mathcal{A}(d\alpha_{22}, 2\beta_{22}) \end{pmatrix}, \tag{8}$$

where d is the dimension ($d = 3$ in the present paper), the α's and β's are constants, and $\mathcal{A}$ stands for a representation of an isotropic fourth rank tensor of the general form

$$\begin{aligned} \{\mathcal{A}(\lambda_1, \lambda_2)\}_{ijkl} &= (\lambda_1/d)\delta_{ij}\delta_{kl} + \frac{1}{2}\lambda_2\left(\delta_{ik}\delta_{jl} + \delta_{il}\delta_{jk} - (2/d)\delta_{ij}\delta_{kl}\right) \\ &= \lambda_1\{\Lambda_h\}_{ijkl} + \lambda_2\{\Lambda_s\}_{ijkl}, \end{aligned} \tag{9}$$

where

$$\{\Lambda_h\}_{ijkl} = \frac{1}{d}\delta_{ij}\delta_{kl} \tag{10}$$

and

$$\{\Lambda_s\}_{ijkl} = \frac{1}{2}\left(\delta_{ik}\delta_{jl} + \delta_{il}\delta_{jk}\right) - \frac{1}{d}\delta_{ij}\delta_{kl} \tag{11}$$

project respectively onto hydrostatic and shear fields. As explained in Part I, the reference tensor is not required to be positive definite, but it is required to be quasiconvex, satisfying

$$\langle \mathbf{e}\cdot\mathbf{D}_0\mathbf{e}\rangle \geq \langle \mathbf{e}\rangle \cdot \mathbf{D}_0 \langle \mathbf{e}\rangle\,, \tag{12}$$

where $\mathbf{e}$ is any periodic field satisfying the constraints on $\mathbf{e}_0$ discussed above. In addition, the reference tensor is chosen to satisfy the standard restrictions

$$\mathbf{D}_1 - \mathbf{D}_0 \geq 0, \qquad \mathbf{D}_2 - \mathbf{D}_0 \geq 0. \tag{13}$$

2.2 General Hashin-Shtrikman bounds

The main Hashin-Shtrikman-type result in the present context is obtained after three more steps of analysis. The first step involves maximizing the left hand side of (5) as a function of $\mathbf{e}_*$ in order to produce the optimal inequality constraint from (5). The value of $\mathbf{e}_*$ that maximizes the left hand side of (5) is easily shown to be (Milton & Kohn 1988; Zhikov 1991 and references therein)

$$\mathbf{e}_* = (\mathbf{D}_0 - \mathbf{D}_*)^{-1}\mathbf{p}_*, \tag{14}$$

where $\mathbf{p}_* = \langle \mathbf{p}(\mathbf{x})\rangle$ is the volume averaged polarization.

In the second step, we consider $\mathbf{p}(\mathbf{x})$ to be piecewise constant and of the form

$$\mathbf{p}(\mathbf{x}) = \mathbf{p}_* - f_1\mathbf{q} + \chi_1(\mathbf{x})\mathbf{q}, \tag{15}$$

where $\mathbf{p}_*$ is the average polarization and therefore a constant, while $\mathbf{q}$ is another constant vector. Since f_1 is the volume fraction of phase 1 and $\chi_1(\mathbf{x})$ is the indicator function for phase 1, we have $f_1 = \langle\chi_1(\mathbf{x})\rangle$ and $\langle\mathbf{p}(\mathbf{x})\rangle = \mathbf{p}_*$ follows from (15), by design with this choice of $\mathbf{p}(\mathbf{x})$. The arbitrariness of $\mathbf{p}(\mathbf{x})$ is inherited by the vector $\mathbf{q}$. Then, it follows immediately from the fact $\langle\mathbf{e}_0\rangle = 0$ that $\mathbf{e}_0$ depends only on the vector $\mathbf{q}$ and not on $\mathbf{p}_*$. Thus, we are free to maximize the left hand side of (5) over $\mathbf{p}_*$, if we choose to do so.

The third step in this process is to find the choice of $\mathbf{p}_*$ that maximizes the left hand side of (5), and thereby eliminate $\mathbf{p}_*$. Having done this, we find that

$$\langle\chi_1(\mathbf{x})\mathbf{q}\cdot\mathbf{e}_0(\mathbf{x})\rangle \geq f_1 f_2 \mathbf{q}\cdot(\mathbf{Y}_* + \mathbf{D}_0)^{-1}\,\mathbf{q}, \tag{16}$$

where $\mathbf{Y}_* = \mathbf{Y}_*(\mathbf{D}_*, \mathbf{D}_1, \mathbf{D}_2)$ is the effective $\mathbf{Y}$-tensor for the composite material, which is given by

$$\mathbf{Y}_*(\mathbf{D}_*, \mathbf{D}_1, \mathbf{D}_2) = \begin{pmatrix} (\mathcal{Y}'')^{-1} & -(\mathcal{Y}'')^{-1}\mathcal{Y}' \\ -\mathcal{Y}'(\mathcal{Y}'')^{-1} & \mathcal{Y}'' + \mathcal{Y}'(\mathcal{Y}'')^{-1}\mathcal{Y}' \end{pmatrix}, \tag{17}$$

where $\mathcal{Y}'$, $\mathcal{Y}''$ are the real and imaginary parts of $\mathcal{Y}(\mathcal{C}_*, \mathcal{C}_1, \mathcal{C}_2)$. The tensor $\mathcal{Y}$ for the viscoelastic problem is given by

$$\mathcal{Y}(\mathcal{C}_*, \mathcal{C}_1, \mathcal{C}_2) = -f_2\mathcal{C}_1 - f_1\mathcal{C}_2 + f_1 f_2(\mathcal{C}_1 - \mathcal{C}_2)(f_1\mathcal{C}_1 + f_2\mathcal{C}_2 - \mathcal{C}_*)^{-1}(\mathcal{C}_1 - \mathcal{C}_2). \tag{18}$$

Equation (16) is the main Hashin-Shtrikman-type result, and so far the analysis has not differed significantly from that contained in Part I.

To make further progress, we need a choice for the reference tensor $\mathbf{D}_0$ and for the constant vector $\mathbf{q}$ that determines the polarization field.

In order to clarify the range of possibilities for the reference tensor $\mathbf{D}_0$, we will at first proceed without making any unnecessary assumptions about its form. But about midway through the analysis, we will specialize the choice so as to obtain bounds constructed in a manner similar to that in Part I, *i.e.*, intersections of circles in the complex plane. It is expected that bounds improving upon the explicit results obtained in this paper could be obtained by following the more general analysis that we present first.

The main issue arising from (16) is how to determine $\mathbf{e}_0$ given choices of $\mathbf{D}_0$ and $\mathbf{q}$. Clearly, $\mathbf{e}_0$ and $\mathbf{j}_0$ reside in orthogonal spaces. Let $\mathbf{\Gamma}_1$ denote a projection operator onto periodic strain fields with vanishing average value, and let $\mathbf{\Gamma}_2$ denote a projection operator onto periodic stress fields with vanishing average value. With these two operators, we construct another operator

$$\tilde{\Gamma} = \begin{pmatrix} \Gamma_2 & 0 \\ 0 & \Gamma_1 \end{pmatrix}, \tag{19}$$

that projects onto fields of the same type as $\mathbf{e}_0$ and is therefore orthogonal to $\mathbf{j}_0$. (It is at this point the present analysis starts to diverge from that of Part I.) Operating on the first equation in (6) with $\tilde{\Gamma}$ and using (15) gives

$$\tilde{\Gamma}\chi_1\mathbf{q} - \tilde{\Gamma}\mathbf{D}_0\mathbf{e}_0 = 0, \tag{20}$$

and, since by definition $\tilde{\Gamma}\mathbf{e}_0 = \mathbf{e}_0$, we also have

$$\tilde{\Gamma}\chi_1\mathbf{q} = \tilde{\Gamma}\mathbf{D}_0\tilde{\Gamma}\mathbf{e}_0. \tag{21}$$

Then we take the formal inverse of the operator on the right of (21) and again make use of the fact that $\tilde{\Gamma}$ is a projection onto the space of $\mathbf{e}_0$ to write the symmetrical form of the result

$$\mathbf{e}_0(\mathbf{x}) = \tilde{\Gamma}\left(\tilde{\Gamma}\mathbf{D}_0\tilde{\Gamma}\right)^{-1}\tilde{\Gamma}\chi_1(\mathbf{x})\mathbf{q}, \tag{22}$$

where the inverse is to be understood as the inverse on the space of fields onto which $\tilde{\Gamma}$ projects. Now substituting into (16), we find

$$\left\langle \mathbf{q}\cdot\chi_1\tilde{\Gamma}\left(\tilde{\Gamma}\mathbf{D}_0\tilde{\Gamma}\right)^{-1}\tilde{\Gamma}\chi_1\mathbf{q}\right\rangle \geq f_1 f_2 \mathbf{q}\cdot\left(\mathbf{Y}_* + \mathbf{D}_0\right)^{-1}\mathbf{q}, \tag{23}$$

which is the desired result, depending only on an arbitrary constant vector $\mathbf{q}$.

To proceed further, we need to know something about the left hand side of (23). Such information is best obtained by representing $\tilde{\Gamma}$ in Fourier space, where it is local. A similar method has been used previously by Milton & Kohn (1988), where more details of the approach may be found. The result (23) holds for every $\mathbf{q}$, so if we have a set of linearly independent $\mathbf{q}_i$'s, we can sum the corresponding set of inequalities to obtain the convenient form

$$\begin{aligned}\sum_i \left\langle \mathbf{q}_i\cdot\chi_1\tilde{\Gamma}\left(\tilde{\Gamma}\mathbf{D}_0\tilde{\Gamma}\right)^{-1}\tilde{\Gamma}\chi_1\mathbf{q}_i\right\rangle &= \sum_i\sum_{\mathbf{k}\neq 0}\mathbf{q}_i\cdot\chi_1(\mathbf{k})\tilde{\Gamma}(\mathbf{k})\left(\tilde{\Gamma}(\mathbf{k})\mathbf{D}_0\tilde{\Gamma}(\mathbf{k})\right)^{-1}\tilde{\Gamma}(\mathbf{k})\chi_1(-\mathbf{k})\mathbf{q}_i \\ &= \sum_{\mathbf{k}\neq 0}\chi_1(\mathbf{k})\chi_1(-\mathbf{k})\mathrm{Tr}\{\mathbf{M}\tilde{\Gamma}(\mathbf{k})\left(\tilde{\Gamma}(\mathbf{k})\mathbf{D}_0\tilde{\Gamma}(\mathbf{k})\right)^{-1}\tilde{\Gamma}(\mathbf{k})\},\end{aligned} \tag{24}$$

where the operator $\mathbf{M}$ is constructed as the sum of the outer products of the $\mathbf{q}_i$s:

$$\mathbf{M} = \sum_i \mathbf{q}_i \otimes \mathbf{q}_i. \tag{25}$$

The operator $\mathbf{M}$ will be chosen so that the trace appearing in (24) is independent of $\mathbf{k}$, for all $\mathbf{k} \neq 0$, in which case the inequality reduces to

$$\sum_{\mathbf{k}\neq 0} \chi_1(\mathbf{k})\chi_1(-\mathbf{k})\mathrm{Tr}\{\mathbf{M}\tilde{\Gamma}\left(\tilde{\Gamma}\mathbf{D}_0\tilde{\Gamma}\right)^{-1}\tilde{\Gamma}\} \geq f_1 f_2 \mathrm{Tr}\{\mathbf{M}\left(\mathbf{Y}_* + \mathbf{D}_0\right)^{-1}\}. \tag{26}$$

Since

$$\sum_{\mathbf{k}\neq 0} \chi_1(\mathbf{k})\chi_1(-\mathbf{k}) = f_1 f_2, \tag{27}$$

equation (26) can finally be rewritten as

$$\mathrm{Tr}\{\mathbf{M}\tilde{\Gamma}\left(\tilde{\Gamma}\mathbf{D}_0\tilde{\Gamma}\right)^{-1}\tilde{\Gamma}\} \geq \mathrm{Tr}\{\mathbf{M}\left(\mathbf{Y}_* + \mathbf{D}_0\right)^{-1}\}. \tag{28}$$

Up to this point in the analysis, we have not specialized to consideration of shear modulus bounds. Indeed, (28) could be used to bound bulk modulus, or shear modulus, or linear combinations. The form (28) is a general statement of the Hashin-Shtrikman-type bounds for the viscoelastic constants with one caveat: Since the Y-tensor has been expressed here in terms of only two constituents through (18), the formula (28) is defined only for composites of two possibly anisotropic phases each with spatially constant orientation. Thus, two-phase polycrystals and multiphase materials are specifically excluded from present consideration. This restriction can be lifted with some additional effort, but (as we will see), since the resulting analysis is already sufficiently involved, it seems best to leave generalizations to future work.

Finally, note the very significant characteristic of (28) that it is independent of the volume fractions and the indicator function χ_1. Thus, a single computation of the bounds on y_μ is sufficient to bound μ_* for the entire range of possible volume fractions.

2.3 General bounds on the shear modulus: Circles in the complex plane

To obtain definite results for the shear modulus, we need to choose some convenient operator $\mathbf{M}$. From (28) it is clear that individual choices of $\mathbf{q}_i$'s are not important, but the overall operator $\mathbf{M}$ is important. We would like to find an $\mathbf{M}$ that makes the computation of the bounds on viscoelastic constants especially simple. In particular, we would like to construct bounds using methods analogous to the ones used in Part I, *i.e.*, intersections of circles in the complex plane (if possible), and that do not depend on additional information such as spatial correlation functions [see, for example, Berryman (1985) for a discussion of methods for quantifying microstructural information and Torquato (1991) for a review of bounding methods making use of such information]. A summary of the analysis required to understand what choices of $\mathbf{M}$ might be appropriate is contained in the Appendix, along with explicit calculation of the left hand side of (28). The key point that motivates the work in this Appendix is that we want to make a choice that decouples the effective bulk response from the effective shear response so that we get bounds directly on the viscoelastic shear modulus. After all, we have already noted that (28) is sufficiently general that it could be used to bound linear combinations of bulk and shear modulus, but we do not want to pursue such possiblities in the present paper.

A specific choice for $\mathbf{M}$ consistent with our goals is found in (12) and may be rewritten as

$$\mathbf{M} = \begin{pmatrix} w_1^2\Lambda_s & w_1 w_2 \Lambda_s \\ w_1 w_2 \Lambda_s & w_2^2 \Lambda_s \end{pmatrix}, \tag{29}$$

where w_1, w_2 are arbitrary scalars. Then, together with the result (13), we can now calculate the right hand side of (28). To do so, we note that the Y-tensor is given explicitly by

$$\mathbf{Y} = \begin{pmatrix} \frac{1}{3y''_\kappa}\Lambda_h + \frac{1}{2y''_\mu}\Lambda_s & -\frac{y'_\kappa}{y''_\kappa}\Lambda_h - \frac{y'_\mu}{y''_\mu}\Lambda_s \\ -\frac{y'_\kappa}{y''_\kappa}\Lambda_h - \frac{y'_\mu}{y''_\mu}\Lambda_s & 3\left[y''_\kappa + \frac{(y'_\kappa)^2}{y''_\kappa}\right]\Lambda_h + 2\left[y''_\mu + \frac{(y'_\mu)^2}{y''_\mu}\right]\Lambda_s \end{pmatrix} \tag{30}$$

where $y_\kappa = y'_\kappa + iy''_\kappa$ and $y_\mu = y'_\mu + y''_\mu$ are related to the complex bulk and shear moduli by

$$y_\kappa = \frac{\kappa_1\kappa_2(\kappa_* < 1/\kappa > -1)}{< \kappa > -\kappa_*}, \tag{31}$$

$$y_\mu = \frac{\mu_1\mu_2(\mu_* < 1/\mu > -1)}{< \mu > -\mu_*}. \tag{32}$$

The standard averages appearing in (31) and (32) are given by

$$\begin{aligned} &< \kappa >= f_1\kappa_1 + f_2\kappa_2, \quad < 1/\kappa >= f_1/\kappa_1 + f_2/\kappa_2, \\ &< \mu >= f_1\mu_1 + f_2\mu_2, \quad < 1/\mu >= f_1/\mu_1 + f_2/\mu_2. \end{aligned} \tag{33}$$

The only unusual feature of (33) is that the material constants, and thus the averages, are complex numbers.

Because this choice of $\mathbf{M}$ is proportional to the shear projection operator Λ_s, only the corresponding terms of $\mathbf{Y}_*$ and $\mathbf{D}_0$ can contribute to the right hand side of (28). Thus, the pertinent part of the sum of these two tensors has the form

$$\mathbf{Y}_* + \mathbf{D}_0 = \begin{pmatrix} \frac{1}{2}\left(\frac{1}{y''_\mu} + \beta_{11}\right)\Lambda_s & \left(-\frac{y'_\kappa}{y''_\kappa} + \beta_{12}\right)\Lambda_s \\ \left(-\frac{y'_\kappa}{y''_\kappa} + \beta_{12}\right)\Lambda_s & 2\left[y''_\mu + \frac{(y'_\mu)^2}{y''_\mu} + \beta_{22}\right]\Lambda_s \end{pmatrix} + \ldots, \tag{34}$$

where the dots indicate irrelevant terms proportional to Λ_h. The final result for the right hand trace is therefore given by

$$\mathrm{Tr}\{\mathbf{M}\,(\mathbf{Y}_* + \mathbf{D}_0)^{-1}\} = 5\,(\, w_1 \quad w_2\,)\,\mathbf{G}^{-1}\begin{pmatrix} w_1 \\ w_2 \end{pmatrix}, \tag{35}$$

where the 2×2 matrix $\mathbf{G}$ is defined by

$$\mathbf{G} = \begin{pmatrix} \frac{1}{2}\left(\frac{1}{y''_\mu} + \beta_{11}\right) & \left(-\frac{y'_\kappa}{y''_\kappa} + \beta_{12}\right) \\ \left(-\frac{y'_\kappa}{y''_\kappa} + \beta_{12}\right) & 2\left[y''_\mu + \frac{(y'_\mu)^2}{y''_\mu} + \beta_{22}\right] \end{pmatrix}. \tag{36}$$

The factor of 5 appearing in (35) arises from the 5×2 degrees of freedom allowed for the shear modes in the 12 dimensional space over which the trace operation is performed.

Comparing (35) with (13) and the trace formula (28) and then recalling the definition (14) of $\mathbf{A}_3$, we find that the bounds imply

$$\mathbf{A}_3^{-1} \geq 5\mathbf{G}^{-1}, \tag{37}$$

or equivalently that

$$\mathbf{G} \geq 5\mathbf{A}_3. \tag{38}$$

We may rearrange this inequality to obtain a relation bounding the submatrix of $\mathbf{G}$ depending on the real and imaginary parts of y_μ. We find that

$$\begin{pmatrix} \frac{1}{2y''_\mu} & -\frac{y'_\mu}{y''_\mu} \\ -\frac{y'_\mu}{y''_\mu} & 2\left[y''_\mu + \frac{(y'_\mu)^2}{y''_\mu}\right] \end{pmatrix} - \mathbf{Z} \geq 0, \tag{39}$$

where

$$\mathbf{Z} \equiv 5\mathbf{A}_3 - \begin{pmatrix} \beta_{11}/2 & \beta_{12} \\ \beta_{12} & 2\beta_{22} \end{pmatrix}. \tag{40}$$

Taking the determinant of the matrix on the left hand side of (39) and noting that this determinant must be nonnegative to satisfy the inequality, we find after some manipulation that

$$\left(y'_\mu + \frac{Z_{12}}{2Z_{11}}\right)^2 + \left(y''_\mu - \frac{1 + Z_{11}Z_{22} - Z_{12}^2}{4Z_{11}}\right)^2 \leq \frac{\left(1 + Z_{12}^2 - Z_{11}Z_{22}\right)^2}{16Z_{11}^2}, \tag{41}$$

showing that the bounding condition is a circle in the complex plane with center at

$$\mathbf{z}_{center} = -\frac{Z_{12}}{2Z_{11}} + i\frac{1 + Z_{11}Z_{22} - Z_{12}^2}{4Z_{11}}, \tag{42}$$

and radius given by

$$R = \frac{|1 + Z_{12}^2 - Z_{11}Z_{22}|}{4|Z_{11}|}. \tag{43}$$

The sought after values of $y_\mu = y'_\mu + iy''_\mu$ must lie inside the specified circle. Thus, the interpretation of the bounds as circles in the complex Y_μ-plane is true, regardless of the specific choices made for parameters α_{11}, α_{12}, α_{22}, β_{11}, β_{12}, and β_{22}.

In addition, similar arguments show that the constraints (13) are themselves circles in the bulk modulus and shear modulus planes. However, the quasiconvexity condition (12) does not share this simple geometric interpretation.

2.4 Simplified shear bounds

Having established that the bounds will be circles in the complex plane, we must now determine which circles in the complex plane. This task is made more difficult than one might expect by the large number of constraints that must be simultaneously satisfied. Rather than treating the most general case, we impose restrictions [see (44)] to ensure that the constraints themselves also have a simple geometrical interpretation. While the resulting bounds might not be the tightest ones that could be extracted from the general theory presented here, they enjoy the advantage of being relatively easy to compute. Furthermore, we show later (see Section 5) that the resulting bounds reduce exactly to the standard Hashin-Shtrikman-Walpole results when all moduli are real.

So, to obtain useful bounds on the complex shear modulus, we must attempt to compute a small bounding region using (39) or equivalently (41), while always simultaneously satisfying the conditions $\mathbf{D}_1 - \mathbf{D}_0 \geq 0$ and $\mathbf{D}_2 - \mathbf{D}_0 \geq 0$ as well as the quasiconvexity condition (12), which place constraints on the parameters in $\mathbf{D}_0$ as specified in (8). As noted in the Appendix, one simplifying assumption we can make is the choice $\alpha_{12} = \beta_{12}$. Then, many of the off-diagonal terms vanish and formulas greatly simplify. This observation suggests that it might prove fruitful to assume the following three relationships:

$$\alpha_{11} = \beta_{11}/c, \quad \alpha_{12} = \beta_{12}, \quad \alpha_{22} = c\beta_{22}, \tag{44}$$

where c is some real, nonnegative constant to be determined. These choices reduce the parameter space for $\mathbf{D}_0$ from six dimensions to four without eliminating any essential features of the bounding problem (as we shall show). Furthermore, it is clear from (12) and (22) that the quasiconvexity condition implies that $\tilde{\Gamma}\mathbf{D}_0\tilde{\Gamma}$ is positive definite, so from (1) it follows that $a_{11,h} > 0$, $a_{22,h} > 0$, $a_{11,s} > 0$, $a_{22,s} > 0$, and $a_{22,h}a_{11,h} - (2/9)(a_{12})^2 > 0$. From (44) and these conditions, it then follows that $\beta_{11} > 0$ and $\beta_{22} > 0$.

With these choices for the α's, the constraints (13) may be rewritten in terms of the following four matrix inequalities:

$$\begin{pmatrix} c/\kappa_j'' - \beta_{11} & \kappa_j'/\kappa_j'' - \beta_{12} \\ \kappa_j'/\kappa_j'' - \beta_{12} & \left[\kappa_j'' + (\kappa_j')^2/\kappa_j''\right]/c - \beta_{22} \end{pmatrix} \geq 0 \quad \text{for} \quad j = 1, 2 \tag{45}$$

and

$$\begin{pmatrix} 1/\mu_j'' - \beta_{11} & \mu_j'/\mu_j'' - \beta_{12} \\ \mu_j'/\mu_j'' - \beta_{12} & \left[\mu_j'' + (\mu_j')^2/\mu_j''\right] - \beta_{22} \end{pmatrix} \geq 0 \quad \text{for} \quad j = 1, 2. \tag{46}$$

Equation (46) is a straightforward restatement of the conditions on the shear terms contained in (13). Equation (45) is obtained from (13) by using in addition the properties of the determinant to show that this is an equivalent form of the result. The form of (45) has been chosen to emphasize the similarities between the sets of equations in (45) and (46).

Next we shall show that the final result for the bounds on the Y-tensor may again be written in the form

$$\begin{pmatrix} \frac{(8+9c)}{6(2+c)y_\mu''} - \beta_{11} & y_\mu'/y_\mu'' - \beta_{12} \\ y_\mu'/y_\mu'' - \beta_{12} & \frac{6(2+c)}{(8+9c)}\left[y_\mu'' + (y_\mu')^2/y_\mu''\right] - \beta_{22} \end{pmatrix} \geq 0. \tag{47}$$

We display this result prior to its derivation to permit easier comparison between this form and those of the constraints on the parameters in (45) and (46). To achieve this particular form, (as we shall see) we have again made use of the properties of determinants to rewrite the bounding equations in an equivalent form that emphasizes the similarities to (45) and (46).

To derive (47), we first substitute (44) into (40) with $\mathbf{A}_3$ given by (14), and then after some algebraic manipulation we find that

$$\mathbf{Z} = \begin{pmatrix} \frac{3(2+c)}{8+9c}\beta_{11} & -\beta_{12} \\ -\beta_{12} & \frac{8+9c}{3(2+c)}\beta_{22} \end{pmatrix}. \tag{48}$$

Substituting (48) into (39), we obtain directly that

$$\begin{pmatrix} \frac{1}{2y''_\mu} - \frac{3(2+c)}{8+9c}\beta_{11} & \beta_{12} - \frac{y'_\mu}{y''_\mu} \\ \beta_{12} - \frac{y'_\mu}{y''_\mu} & 2\left[y''_\mu + \frac{(y'_\mu)^2}{y''_\mu}\right] - \frac{8+9c}{3(2+c)}\beta_{22} \end{pmatrix} \geq 0. \tag{49}$$

This result can then be shown to be equivalent to (47) using the fact the nonnegativity of a 2×2 matrix implies that the diagonal elements are nonnegative, and that the determinant is also nonnegative. First, the signs of both off-diagonal terms can be simultaneously reversed because this does not change the determinant. Then, the numerical factors multiplying β_{11} and β_{22} can be shifted by noting that multiplying the first diagonal element by $(8+9c)/3(2+c)$ and the second by $3(2+c)/(8+9c)$ also has no effect on the determinant. This step is equivalent to making a change of basis by multiplying the matrix on the left and right by a diagonal matrix of the form

$$\begin{pmatrix} k & 0 \\ 0 & -1/k \end{pmatrix}, \tag{50}$$

where $k = \sqrt{(8+9c)/3(2+c)}$. As long as these numerical factors are real, then the positivity of the diagonal elements also remains unaffected. This completes the derivation of (47).

Now that we have an explicit expression for $\mathbf{Z}$ in (48), we can return to (42) and (43) to show that

$$R^2 < |\mathbf{z}_{center}|^2, \tag{51}$$

if $0 < Z_{11}Z_{22}$. But the quasiconvexity condition shows that $\beta_{11} > 0$ and $\beta_{22} > 0$, so it follows from (48) that $Z_{11} > 0$ and $Z_{22} > 0$. Therefore, (51) is true for the choice of parameterization (44). Inequality (51) implies that the bounding circles for y_μ never contain the origin.

The main result of this paper for applications of viscoelastic shear modulus bounds is contained in equations (45)-(47). The remainder of the paper will be devoted to explaining and then evaluating these bounds. A somewhat more convenient form of the constraints and bounds is obtained in the next section. Then, after summarizing the remaining steps in the analysis in the intervening Sections, a concise statement of the resulting algorithm is presented in Section 7.

3 Description and significance of the bounds

The form of the equations in (45)-(47) has been carefully chosen so it is easy to describe both the bounds themselves and the parameter constraints that give rise to the bounds using the same language, *i.e.*, descriptions of particular circles in the complex plane. In addition to the quasiconvexity constraints showing that $\beta_{11} > 0$ and $\beta_{22} > 0$, there are five sets of inequalities in (45)-(47). Each of these sets reduces to two inequalities: one on the leading diagonal component of the matrices and one on the determinant. (The positivity of the determinant and one diagonal element implies the positivity of the remaining diagonal element.) We will concentrate first on explaining the significance of all the determinants.

3.1 Determinant inequalities and quasiconvexity

The simplest examples are those for the shear modulus constraints (46), which can then be understood as generic for all the constraints and bounds. Computing the determinant for $j = 1$, we find that the complex number $\mu_1' + i\mu_1''$ must lie inside or on the boundary of a circle in the complex plane with center given by

$$x_0 + iy_0 = \frac{\beta_{12}}{\beta_{11}} + i\frac{1 + \beta_{11}\beta_{22} - \beta_{12}^2}{2\beta_{11}}, \tag{1}$$

and radius given by

$$R = \frac{|1 + \beta_{12}^2 - \beta_{11}\beta_{22}|}{2\beta_{11}}. \tag{2}$$

To satisfy all the constraints simultaneously, the same circle (as determined by the β's) must contain not only μ_1, but also μ_2, κ_1/c, and κ_2/c. The theory then shows (assuming all the remaining constraints are satisfied simultaneously) that any such circle containing all four of these points must also contain a scaled version of the desired point y_μ with scale factor $6(2+c)/(8+9c)$. Thus, any such circle must serve as a bounding circle for the effective shear modulus via an appropriate transformation from the pertinent complex plane.

The preceding discussion is fine for fixed values of c, but this parameter should be varied to obtain the best possible bound. If we do not alter the preceding analysis, the significance of the complex plane where the bounds are computed will change with every choice of c. To avoid this nontrivial complication, we will again use the scaling properties of the matrix inequalities to rewrite them all in the same convenient form:

$$\begin{pmatrix} 1/y_\mu'' - \frac{6(2+c)}{8+9c}\beta_{11} & y_\mu'/y_\mu'' - \beta_{12} \\ y_\mu'/y_\mu'' - \beta_{12} & \left[y_\mu'' + (y_\mu')^2/y_\mu''\right] - \frac{8+9c}{6(2+c)}\beta_{22} \end{pmatrix} \geq 0, \tag{3}$$

with the constraint equations becoming

$$\begin{pmatrix} \frac{6c(2+c)}{(8+9c)\kappa_j''} - \frac{6(2+c)}{8+9c}\beta_{11} & \kappa_j'/\kappa_j'' - \beta_{12} \\ \kappa_j'/\kappa_j'' - \beta_{12} & \frac{8+9c}{6c(2+c)}\left[\kappa_j'' + (\kappa_j')^2/\kappa_j''\right] - \frac{8+9c}{6(2+c)}\beta_{22} \end{pmatrix} \geq 0 \quad \text{for} \quad j = 1, 2 \tag{4}$$

and

$$\begin{pmatrix} \frac{6(2+c)}{(8+9c)\mu_j''} - \frac{6(2+c)}{8+9c}\beta_{11} & \mu_j'/\mu_j'' - \beta_{12} \\ \mu_j'/\mu_j'' - \beta_{12} & \frac{8+9c}{6(2+c)}\left[\mu_j'' + (\mu_j')^2/\mu_j''\right] - \frac{8+9c}{6(2+c)}\beta_{22} \end{pmatrix} \geq 0 \quad \text{for} \quad j = 1, 2. \tag{5}$$

Now the parameters

$$\frac{6(2+c)}{8+9c}\beta_{11}, \quad \beta_{12}, \quad \frac{8+9c}{6(2+c)}\beta_{22} \tag{6}$$

play the role previously played by β_{11}, β_{12}, β_{22}, respectively. The bounds on y_μ are still exactly the same, but now for each choice of the parameter c a single circle contains all four constraining points:

$$\gamma(c)\mu_j \quad \text{and} \quad \gamma(c)\kappa_j/c \quad \text{for} \quad j = 1, 2, \tag{7}$$

where

$$\gamma(c) \equiv \frac{8+9c}{6(2+c)}, \tag{8}$$

together with the desired y_μ point in the *fixed* Y_μ-plane. Thus, for every choice of the parameter c, we may seek a set of the most constraining circles that contain all four of these constraint points, while excluding the origin — as required by the condition of quasiconvexity. Then, as we vary the parameter c and consider the intersections of all such circles in the Y_μ-plane, the desired bounding curve is finally obtained as the boundary of the intersection set (*i.e.*, the convex hull) of this infinite set of circles.

In general, bounds on the viscoelastic shear modulus can be obtained fairly easily using the method just described. However, we show in Sections 6 and 7 that more can be said about the convex hull generated by this method.

3.2 Diagonal element inequalities

So far we have treated only the determinant constraints from the bounding relations (3)-(5) together with the constraints from quasiconvexity. In addition to these constraints, there are also nonnegativity constraints on the diagonal components of these matrices. What then is the significance of these further constraints?

Since the determinant inequality for the circle guarantees that the product of the two diagonal elements of each matrix is positive, it will be sufficient for us to prove that one of the diagonal elements is positive for each matrix; then the other diagonal element must also be positive. To achieve this result, we need to find a geometric interpretation of the β's. If the circle containing the four constraining points has center at $\mathbf{z}_0 = x_0 + iy_0$ and the radius of the circle is R, then it is not hard to invert the formulas (1) and (2) for the β's. Two of the β's may be related to the third by the general formulas $\beta_{12} = x_0\beta_{11}$ and $\beta_{22} = (x_0^2 + y_0^2 - R^2)\beta_{11}$. Thus, if $\beta_{11} > 0$, then $\beta_{22} > 0$ whenever the circle excludes the origin, *i.e.*, whenever $x_0^2 + y_0^2 > R^2$, which follows from quasiconvexity. A fourth order equation determines β_{11}. This equation has four real roots, two of which are positive and two negative. Of these four roots, two are pertinent to the circle of interest, while the other two are pertinent to another circle obtained by rotating the complex plane through π radians. Of the two distinct values of β_{11} for the bounding circle, the one of interest is the one producing the smallest positive value of β_{11} and that is

$$\beta_{11} = \frac{1}{y_0 + R}, \tag{9}$$

which is necessarily always positive when the circle contains moduli with positive imaginary parts. This result has a simple geometric interpretation: The highest point of the bounding circle in the complex plane is located at $x_0 + i(y_0 + R)$. Thus, $1/\beta_{11}$, as determined by (9), is an upper bound on the imaginary parts of all points lying within the circle. Then, it follows easily from (4) and (5) that the first diagonal element of each of these matrices is nonnegative. Combining this result with the determinant inequality is sufficient to prove that both diagonal constraints are satisfied for this choice (9) of β_{11}. Thus, (9) guarantees satisfaction of all the diagonal constraints for any circle containing the constraining points.

If $y_0 > R$, the other positive choice of β_{11} is given by $\beta_{11} = 1/|y_0 - R|$. This choice also has a simple geometric interpretation since in this case $1/\beta_{11}$ will be a lower bound on the imaginary parts of all points lying inside the circle. Thus, for this case both diagonal elements of each matrix will be negative. This choice of β_{11} is therefore excluded by the diagonal constraints. If $y_0 < R$, the other choice of β_{11} associated with this circle is $\beta_{11} = -1/|y_0 - R| < 0$, which is excluded by the quasiconvexity constraint.

These results imply that the diagonal constraints in (4)-(5) affect only the specific values of the β's and have no other influence on the validity of the circles obtained from (3) as bounds on y_μ. Thus, if we concentrate on the geometrical interpretation of the constraints and bounds as circles in the complex plane that exclude the origin, we can completely ignore the β's. The nonnegativity constraints on the diagonal elements need not be considered further as we develop the general algorithm for constructing the convex hull of shear modulus bounds.

4 A simple example

We will find that the general algorithm for constructing the bounds on viscoelastic shear moduli is somewhat complicated. Before attempting to explain the method in its full generality, it may prove enlightening for the reader to see a simple example of the application of the bounding formulas. To this end, we first consider an example with $(\kappa_1, \mu_1) = (i\,6.0, i\,3.0)$ and $(\kappa_2, \mu_2) = (10.0, 5.0)$. This example is qualitatively very similar to one first considered by Gibiansky & Lakes (1993). This example is chosen for illustrative purposes because of the simplifying property that when the bulk moduli are scaled by a factor $c = 2.0$, the four points (one for each of the four moduli) in the complex plane coalesce into only two points, one on the real axis and one on the imaginary axis. The optimum bounding region is determined by the two limiting circles that pass through these two points and also through either the origin or through infinity. The circle with its third determining point at infinity results in a straight line between the two points. The circle passing through the origin provides the optimum bounding arc to close the bounding region (*i.e.*, any other circle that includes the two points and excludes the origin will contain the resulting bounding region as a subset). Then, we are led to the particularly simple bounding region shown in the Figure 2 in the Y_μ-plane. Figure 3 shows how the bounds on μ are subsequently constructed in the μ-plane from the information obtained in the Y_μ-plane, assuming a 50/50 concentration of the two constitutents.

In addition to the bounding curves, each of these Figures also shows four special points in the complex plane. We call these points the Hashin-Shtrikman-Walpole points. Defining the function of two complex variables $y(\kappa, \mu) \equiv (\mu/6)(9\kappa + 8\mu)/(\kappa + 2\mu)$, the locations of these points in the Y_μ-plane are found to be:

$$y_1 \equiv y(\kappa_1, \mu_1) = (\mu_1/6)(9\kappa_1 + 8\mu_1)/(\kappa_1 + 2\mu_1), \tag{1}$$

$$y_2 \equiv y(\kappa_2, \mu_2) = (\mu_2/6)(9\kappa_2 + 8\mu_2)/(\kappa_2 + 2\mu_2), \tag{2}$$

$$y_3 \equiv y(\kappa_2, \mu_1) = (\mu_1/6)(9\kappa_2 + 8\mu_1)/(\kappa_2 + 2\mu_1), \tag{3}$$

$$y_4 \equiv y(\kappa_1, \mu_2) = (\mu_2/6)(9\kappa_1 + 8\mu_2)/(\kappa_1 + 2\mu_2). \tag{4}$$

Thus, these points are just the four possible combinations obtainable from substituting the constitutent values for κ and μ in the formula for $y(\kappa, \mu)$.

These values do not yet appear to play a special role in the general formulation of the theory for the viscoelastic shear modulus bounds, but in the limit of all real moduli (or when all moduli lie along a single ray through the origin in the complex μ-plane) they do play an important role in the Hashin-Shtrikman-Walpole bounds (Hashin & Shtrikman, 1963; Walpole, 1966). Also, the related points in the Y_κ-plane do play a role in the theory for the bulk modulus bounds, as has been shown previously in Part I. In the cases studied so far, it has been found that all four Hashin-Shtrikman-Walpole points always lie either inside or on the boundary of the best viscoelastic shear modulus bounds we have found. Furthermore, we show in the next section that the bounds derived here reduce to the Hashin-Shtrikman-Walpole bounds when all constituent moduli are real. In general, it is not expected that all four of these points will necessarily lie inside truly optimum bounds. (Since only a part of the allowed parameter space is being explored, optimality of the resulting bounds is not expected.) It is known from previous work of Milton and Phan-Thien (1982) that the Walpole bounds can be improved and are therefore not realizable, which suggests that y_3 and y_4 might not always lie inside optimal bounds. Also, since we show in the next section that our results reduce to the nonoptimal Walpole bounds when the moduli are real with $(\kappa_1 - \kappa_2)(\mu_1 - \mu_2) < 0$, the present bounds are surely not optimal. On the other hand, the first two points (y_1 and y_2) have been shown to correspond to realizable microstructures by Lurie and Cherkaev (1984), Norris (1985), Francfort and Murat (1986), and Milton (1986), so it is expected these two points should always lie inside the bounds.

The reason for the simplicity of this example lies in the fact that for this choice of constitutent parameters there exists a unique value of the scaling parameter c such that the four points coalesce into only two in the complex Y_μ-plane. To achieve the simple result, it is not important where those two points lie in the complex Y_μ-plane, but it is important that there are only two points. This occurs when both phases share the same Poisson's ratio and the Poisson's ratio is real; then, for this well-ordered case, the corners of the lens-shaped region in the complex Y_μ-plane are located at the Hashin-Shtrikman points y_1 and y_2. It also occurs in the badly-ordered case when the ratios κ_1/μ_2 and κ_2/μ_1 are real and equal; then the corners of the lens-shaped region are located at the Walpole points y_3 and y_4. Gibiansky, Lakes, & Milton (1993) found similar lens-shaped bounding regions for the complex shear modulus in the two-dimensional problem assuming a constraint that is valid in particular when the Poisson's ratios of the two phases were real and equal.

5 Limiting behavior for real moduli

To clarify the relationship between the present results and those of previous authors, it is important to check whether our results reduce to the well-known Hashin-Shtrikman-Walpole bounds (Hashin & Shtrikman, 1963; Walpole, 1966) in the limit when all constituent moduli are real. We show that this is indeed the case in this section.

When all the moduli are real, it is convenient to introduce some new notation. Let $\kappa_- = \min(\kappa_1, \kappa_2)$, $\kappa_+ = \max(\kappa_1, \kappa_2)$, $\mu_- = \min(\mu_1, \mu_2)$, and $\mu_+ = \max(\mu_1, \mu_2)$. Similarly, Y^- and Y^+ will denote the lower and upper bounds in the Y_μ-plane along the real axis.

Now if we consider all possible circles in the complex plane that contain the four points (7), it is clear that the lower bound Y^- can only depend on $\gamma(c)\kappa_-/c$ and $\gamma(c)\mu_-$, while the upper bound Y^+ can depend only on $\gamma(c)\kappa_+/c$ and $\gamma(c)\mu_+$. For each particular choice of indexing parameter c, it is clear that the optimum circle is determined by the minimum in the first instance and by the maximum in the second. Then, as we consider all possible circles, it is also clear that the optimum bounds are obtained by taking the maximum of the minima and the minimum of the maxima, respectively. We write these results as

$$Y^- = \max_{0 \le c \le \infty} \min[\gamma(c)\kappa_-/c, \gamma(c)\mu_-] \tag{1}$$

and

$$Y^+ = \min_{0 \le c \le \infty} \max[\gamma(c)\kappa_+/c, \gamma(c)\mu_+]. \tag{2}$$

The factors $\gamma(c)$ and $\gamma(c)/c$ are both monotonic functions of c: as c varies from 0 to ∞, $\gamma(c)$ increases from 2/3 to 3/2, while $\gamma(c)/c$ decreases from ∞ to 0. Thus, for example,

$$\min[\gamma(c)\kappa_-/c, \gamma(c)\mu_-] = \begin{cases} \gamma(c)\mu_- & \text{for } 0 \le c \le \kappa_-/\mu_- \\ \gamma(c)\kappa_-/c & \text{for } \kappa_-/\mu_- \le c \le \infty. \end{cases} \tag{3}$$

Furthermore, since the scaling factors are monotonic, the maximum of (3) clearly occurs when the points cross at $c = \kappa_-/\mu_-$. A similar argument for Y^+ shows that the bounds are given by

$$Y^- = \gamma(\kappa_-/\mu_-)\mu_- \tag{4}$$

and

$$Y^+ = \gamma(\kappa_+/\mu_+)\mu_+. \tag{5}$$

But, when transformed to the μ-plane, these results are precisely the Hashin-Shtrikman-Walpole bounds, which is what we had hoped to show.

Note that a similar result also applies whenever all four moduli lie on a single ray (regardless of angle) through the origin of the complex plane.

6 General algorithm for constructing the convex hull

To illustrate the type of bounds generated for fixed values of c, we consider the value $c = 1$ for which results are shown as the dashed lines in Figure 4 (a more complete discussion of this example follows at the end of this section). As can be seen in this example, the relevant "circles" are half planes containing the four points in Eq. (7) but not containing the origin, and circles containing the four points and passing through the origin. (The four solid dots in this figure are again the Hashin-Shtrikman-Walpole points (1)–(4), included as a visual aid.) Although such bounds for fixed values of c can be useful in themselves, it would clearly be advantageous if we could find a general means of constructing the best possible bounds within our present constraints. Such a construction is now derived in this section.

6.1 Legendre transform approach for the general algorithm

We now consider the general problem of finding the intersection of all circles in the complex Y_μ-plane containing the four points in Eq. (7) (but not containing the origin) for some real non-negative value of c. Let B denote this region of intersection.

Let B^- denote the region of intersection of all half planes in the complex Y_μ-plane containing the four points (but not containing the origin) for some real non-negative value of c. Let B^+ denote the region of intersection of all circles passing through (actually just grazing) the origin that contain the four points for some real non-negative value of c. Clearly, the final bounding set B is just the intersection of the these two regions, so we have

$$B = B^- \cap B^+. \tag{1}$$

Inner boundary

Let us first focus on finding the boundary ∂B^-, which we call the "inner boundary," of the region B^-. Since B^- is a convex set and moreover the region of intersection of half-planes, the boundary of this set is conveniently characterized by its Legendre transform. To avoid technicalities, it is convenient to assume initially — by making a rotation of the complex plane if necessary — that the real parts of $\kappa_1, \kappa_2, \mu_1$ and μ_2 do not all share the same sign and that their imaginary parts are all positive. (Before making such a rotation of the complex plane, their imaginary parts are necessarily always of the same sign because the energy dissipation into heat must always be positive.) Then, the boundary ∂B^- can be described by a single-valued function f^- such that

$$y = f^-(x) \quad \text{if and only if} \quad z^- = x + iy \in \partial B^-. \tag{2}$$

Let us define $h^-(m)$ as the Legendre transform of $f^-(x)$:

$$h^-(m) = \sup_x [mx - f^-(x)]. \tag{3}$$

Here $-h^-(m)$ has a geometrical interpretation as the intercept along the y-axis of a line with slope m that is tangent to the graph $y = f^-(x)$.

To compute this Legendre transform for a given value of m, it suffices to consider the four points and take the infimum over all values of c, giving

$$h^-(m) = \inf_{c \geq 0} \gamma(c) \max[(m\kappa_1' - \kappa_1'')/c, (m\kappa_2' - \kappa_2'')/c, m\mu_1' - \mu_1'', m\mu_2' - \mu_2''], \tag{4}$$

unless the answer of this calculation happens to be positive in which case we set

$$h^{-}(m) = \infty. \tag{5}$$

Eq. (5) reflects the fact that we are only considering half-planes that do not contain the origin, *i.e.*, those half-planes that have positive intercept along the y-axis. Thus, the function $h^{-}(m)$ is finite only in the interval

$$m_L \leq m \leq m_U, \tag{6}$$

where

$$\begin{aligned} m_L &= \min\{\kappa_1''/\kappa_1', \kappa_2''/\kappa_2', \mu_1''/\mu_1', \mu_2''/\mu_2'\} < 0, \\ m_U &= \max\{\kappa_1''/\kappa_1', \kappa_2''/\kappa_2', \mu_1''/\mu_1', \mu_2''/\mu_2'\} > 0. \end{aligned} \tag{7}$$

[The inequalities in (7) follow from the assumed rotation of the complex plane in this approach.] Defining

$$\mu_i = \mu_i' + i\mu_i'' = \mu_1 \quad \text{if} \quad m\mu_1' - \mu_1'' \geq m\mu_2' - \mu_2'' \tag{8}$$

with $\mu_i = \mu_2$ otherwise, and

$$\kappa_j = \kappa_j' + \kappa_j'' = \kappa_1 \quad \text{if} \quad m\kappa_1' - \kappa_1'' \geq m\kappa_2' - \kappa_2'' \tag{9}$$

with $\kappa_j = \kappa_2$ otherwise, and setting

$$c_1 = c_1(m) = \frac{m\kappa_j' - \kappa_j''}{m\mu_i' - \mu_i''}, \tag{10}$$

the above expression for $h^{-}(m)$ reduces to

$$\begin{aligned} h^{-}(m) &= \gamma(c_1)[m\mu_i' - \mu_i''] \quad \text{when} \quad m_L \leq m \leq m_U \\ &= \infty \quad \text{otherwise.} \end{aligned} \tag{11}$$

The actual boundary $y = f^{-}(x)$ can now be recovered from $h^{-}(m)$ by using the inverse Legendre transform :

$$f^{-}(x) = \sup_m [mx - h^{-}(m)]. \tag{12}$$

The supremum over m in this expression is attained when m is such that

$$\begin{aligned} x &= \frac{dh^{-}(m)}{dm} = \mu_i'\gamma(c_1) + (\kappa_j' - c_1\mu_i')\frac{d\gamma(c_1)}{dc_1} \\ &= \frac{\mu_i'(8 + 9c_1)}{6(2 + c_1)} + \frac{5(\kappa_j' - c_1\mu_i')}{3(2 + c_1)^2}, \end{aligned} \tag{13}$$

where we have assumed that at this value of m the curve $h^{-}(m)$ is smooth enough to have one derivative and $m_L \leq m \leq m_U$. The value of the supremum is

$$y = mx - h^{-}(m) = mx - \gamma(c_1)[m\mu_i' - \mu_i''] \tag{14}$$

Consequently the associated value of $z^-(m) = x + iy$ is

$$\begin{aligned} z^-(m) &= (\mu_i' + i\mu_i'')\gamma(c_1) + (1+im)(\kappa_j' - c_1\mu_i')\frac{d\gamma(c_1)}{dc_1} \\ &= \mu_i\gamma(c_1) + (\kappa_j - c_1\mu_i)\frac{d\gamma(c_1)}{dc_1} \\ &= \frac{\mu_i(8+9c_1)}{6(2+c_1)} + \frac{5(\kappa_j - c_1\mu_i)}{3(2+c_1)^2}. \end{aligned} \tag{15}$$

This expression for $z^-(m)$ can be rewritten as a linear combination of $\gamma(c_1)\mu_i$ and $\gamma(c_1)\kappa_j/c_1$:

$$z^-(m) = [p(c_1)\mu_i + [1 - p(c_1)]\kappa_j/c_1]\,\gamma(c_1) \quad \text{where} \quad p(c) = 1 - \frac{c}{\gamma(c)}\frac{d\gamma(c)}{dc}. \tag{16}$$

Thus, these particular points on the boundary of B^- lie on the line joining $\gamma(c)\mu_i$ and $\gamma(c)\kappa_j/c$.

It may happen that the values of either μ_i or κ_j switch from the one possible choice to the other as m is increased. At any critical value $m = m_c$ where such a change occurs, the function $h(m)$ will be continuous but will have a discontinity in its slope. The Legendre transform $f^-(x)$ will have an associated straight line segment in its boundary. According to whether the change is in the value of μ_i or κ_j, this straight line segment lies either along the line joining $\gamma(c_c)\mu_1$ with $\gamma(c_c)\mu_2$ or along the line joining $\gamma(c_c)\kappa_1/c_c$ with $\gamma(c_c)\kappa_2/c_c$ where $c_c = c(m_c)$ and $c(m)$ is given by (10).

The prescription for obtaining the boundary of B^- is as follows. For m continuously increasing from m_L to m_U given by (7), first compute the values of μ_i, κ_j, $c_1(m)$ according to (8), (9) and (10) and plot the points $z^-(m)$ given by (15) in the complex plane. When m reaches any critical point m_c where the value of μ_i or κ_j changes, the curves for $m < m_c$ and for $m > m_c$ should be joined by a straight line segment. Finally, the boundary should be completed for large positive values of x by the ray

$$z^- = z^-(m_U) + t(1/m_U + i) \quad \text{as } t \text{ varies from 0 to } \infty \tag{17}$$

directed outward from the point $z^-(m_U)$. Similarly, the boundary should be completed for large negative values of x by the ray

$$z^- = z^-(m_L) + t(1/m_L + i) \quad \text{as } t \text{ varies from 0 to } \infty \tag{18}$$

directed outward from the point $z^-(m_L)$. Note that, if the formulas (17) and (18) are used in computer algorithms, special care must be exercised if m_U and m_L are zero and/or infinite, *i.e.*, for horizontal or vertical rays.

When the real parts of $\kappa_1, \kappa_2, \mu_1$ and μ_2 share the same sign then the same basic prescription still holds. The only difference is that the definitions of m_L and m_U need to be generalized to

$$\frac{1}{m_L} \equiv \min\left[\frac{\kappa_1'}{\kappa_1''}, \frac{\kappa_2'}{\kappa_2''}, \frac{\mu_1'}{\mu_1''}, \frac{\mu_2'}{\mu_2''}\right], \tag{19}$$

and

$$\frac{1}{m_U} \equiv \max\left[\frac{\kappa_1'}{\kappa_1''}, \frac{\kappa_2'}{\kappa_2''}, \frac{\mu_1'}{\mu_1''}, \frac{\mu_2'}{\mu_2''}\right], \tag{20}$$

Notice that m_L is in fact greater than m_U when the real parts of $\kappa_1, \kappa_2, \mu_1$ and μ_2 share the same sign. Accordingly, starting from $m = m_L$, one computes $z^-(m)$ while increasing m to $m = \infty$ and then m is increased from $-\infty$ to m_U. At each value of m, we select the moduli according to (8) and (9). Any breaks in the curve $z^-(m)$ (which occur when the value of μ_i or κ_j changes) are joined by straight line segments and the rays (17) and (18) are drawn outwards from the points $z^-(m_L)$ and $z^-(m_U)$. This completes the description of the algorithm for constructing the boundary of B^-.

Outer boundary

An analogous argument can be applied to determine the boundary ∂B^+, which we call the "outer boundary," of B^+. Working in the reciprocal $1/Y_\mu$ complex plane, circles in the Y_μ-plane containing the four points $\gamma(c)\mu_1$, $\gamma(c)\mu_2$, $\gamma(c)\kappa_1/c$ and $\gamma(c)\kappa_2/c$ and passing through the origin correspond to half planes in the $1/Y_\mu$-plane that contain the four points $1/(\gamma(c)\mu_1)$, $1/(\gamma(c)\mu_2)$, $c/(\gamma(c)\kappa_1)$ and $c/(\gamma(c)\kappa_2)$, but which do not contain the origin.

To obtain the boundary of B^+ in the Y_μ-plane, we introduce the inverse moduli (the compliances)

$$\begin{aligned} \tilde{\mu}_1 &= \tilde{\mu}_1' + i\tilde{\mu}_1'' = 1/\mu_1, \quad \tilde{\mu}_2 = \tilde{\mu}_2' + i\tilde{\mu}_2'' = 1/\mu_2, \\ \tilde{\kappa}_1 &= \tilde{\kappa}_1' + i\tilde{\kappa}_1'' = 1/\kappa_1, \quad \tilde{\kappa}_2 = \tilde{\kappa}_2' + i\tilde{\kappa}_2'' = 1/\kappa_2, \end{aligned} \tag{21}$$

and define

$$\frac{1}{n_L} \equiv \min\left[\frac{\tilde{\kappa}_1'}{\tilde{\kappa}_1''}, \frac{\tilde{\kappa}_2'}{\tilde{\kappa}_2''}, \frac{\tilde{\mu}_1'}{\tilde{\mu}_1''}, \frac{\tilde{\mu}_2'}{\tilde{\mu}_2''}\right] = -\frac{1}{m_U} \tag{22}$$

and

$$\frac{1}{n_U} \equiv \max\left[\frac{\tilde{\kappa}_1'}{\tilde{\kappa}_1''}, \frac{\tilde{\kappa}_2'}{\tilde{\kappa}_2''}, \frac{\tilde{\mu}_1'}{\tilde{\mu}_1''}, \frac{\tilde{\mu}_2'}{\tilde{\mu}_2''}\right] = -\frac{1}{m_L}. \tag{23}$$

Then, by analogy to (16), we find that by starting from $n = n_L = -m_U$ and increasing n, we may plot the curve in the Y_μ-plane determined by

$$\begin{aligned} z^+(n) &= \left[\frac{1}{\mu_k\gamma(c_2)} + \frac{c_2}{[\gamma(c_2)]^2}\frac{d\gamma(c_2)}{dc_2}\left(\frac{c_2}{\kappa_\ell} - \frac{1}{\mu_k}\right)\right]^{-1} \\ &= \left[\frac{6(2+c_2)}{\mu_k(8+9c_2)} + \frac{60c_2}{(8+9c_2)^2}\left(\frac{c_2}{\kappa_\ell} - \frac{1}{\mu_k}\right)\right]^{-1} \end{aligned} \tag{24}$$

where, in terms of the inverse moduli (the compliances),

$$c_2 = c_2(n) = \frac{n\tilde{\mu}_k' - \tilde{\mu}_k''}{n\tilde{\kappa}_\ell' - \tilde{\kappa}_\ell''} \tag{25}$$

and

$$\mu_k = 1/(\tilde{\mu}_k' + i\tilde{\mu}_k'') = \mu_1 \quad \text{if} \quad n\tilde{\mu}_1' - \tilde{\mu}_1'' \leq n\tilde{\mu}_2' - \tilde{\mu}_2'', \tag{26}$$

with $\mu_k = \mu_2$ otherwise, and

$$\kappa_\ell = 1/(\tilde{\kappa}_j' + \tilde{\kappa}_j'') = \kappa_1 \quad \text{if} \quad n\tilde{\kappa}_1' - \tilde{\kappa}_1'' \leq n\tilde{\kappa}_2' - \tilde{\kappa}_2'', \tag{27}$$

with $\kappa_\ell = \kappa_2$ otherwise. If $n_L < n_U$, then the process stops when $n = n_U = -m_L$. Otherwise n increases to ∞ and then increases from $-\infty$ to terminate at $n = n_U$. Any breaks in the resulting curve $z^+(n)$ (which occur when the value of μ_k or κ_ℓ changes) are joined by circular arcs which — when extended — pass through the origin. Finally, the boundary of B^+ is completed by two circular arcs extending inwards to the origin from the points $z^+(n_U)$ and $z^+(n_L)$. In particular,

$$z^+ = [1/z^+(n_U) - t(1/n_U + i)]^{-1} \quad \text{as } t \text{ varies from 0 to } \infty \tag{28}$$

and

$$z^+ = [1/z^+(n_L) - t(1/n_L + i)]^{-1} \quad \text{as } t \text{ varies from 0 to } \infty. \tag{29}$$

Again note that, if these two equations are used to develop computer codes, special care will be required to treat cases with zero and/or infinite values of n_L and n_U.

As we shall see in the next section, it proves convenient to to parameterize the boundaries of B^- and B^+ by a single variable

$$\theta = \tan^{-1}(m), \quad \text{and} \quad \theta = -\tan^{-1}(n) \tag{30}$$

respectively, rather than using the tangents m and n themselves.

6.2 Example

As an example of this construction consider the case $(\kappa_1, \mu_1) = (2/3 + i/3, 1/2 + i\sqrt{3}/2)$ and $(\kappa_2, \mu_2) = (5/3 + i\,5/6, 1 + i\sqrt{3})$. This example has not been considered in previous work. It was chosen to highlight the situation in which the two pairs of the moduli (*i.e.*, the two shear moduli and the two bulk moduli) lie along two rays in the complex plane. Since $\mu_2/\mu_1 = 2$ is a positive real number, the two shear moduli lie along one ray through the origin ($\tan\theta = \sqrt{3}$), while, since $\kappa_2/\kappa_1 = 5/2$, the two bulk moduli lie along another ray through the origin ($\tan\theta = 1/2$). Consequently, the values of μ_i and κ_j given by (8) and (9) remain equal to μ_1 and κ_1, respectively, for all m between m_L and m_U, while the values of μ_k and κ_ℓ given by (26) and (27) remain equal to μ_2 and κ_2, respectively, for all n between n_L and n_U. Values of c cover the full range from 0 to ∞ as m and n vary between their limiting values for this example, but in other examples c may have a more restricted range since the limiting values of m and n can correspond to finite nonzero c's. For the inner boundary ∂B^- of the curve in Figure 4, we consider (15) with $i = 1$ and $j = 1$. For the outer boundary ∂B^+ of the curve in Figure 4, we consider (24) with $k = 2$ and $\ell = 2$. These two pieces constitute the entire boundary of the convex hull for this problem since they either meet at a point, or cross to close the figure.

Results obtained using the comparatively crude bounds for $c = 0$ and ∞ are shown as the dashed lines in Figure 5. In this case, because the two μ's lie on the same ray in Figure 5, the upper most straight line is a legitimate bounding line since it corresponds to a circle whose third point lies at infinity anywhere to the right of the line. Similarly, because the two bulk moduli are on the same ray, the lower most straight line in Figure 5 corresponds to a circle through the two bulk modulus points and closed at infinity anywhere to the left of the line. The arc of the circle shown in Figure 5 is obtained considering a circle that passes through the origin and also through the two outer most points $\gamma(c)(1 + i\,\sqrt{3})$ and $\gamma(c)(5/3 + i\,5/6)/c$ (thus automatically containing the other two required points). Taking the limit as $c \to \infty$, the outer most bulk modulus point converges to the origin and the circle in question becomes tangent to the ray on which the two bulk moduli lie ($\tan\theta = 1/2$) at the origin. The arc in Figure 5 is precisely the one that passes through the origin, through the point $(3/2)(1+i\sqrt{3})$, and is in addition tangent to the ray of the bulk moduli at the origin.

The comparison shown in Figure 5 of the rather crude results for $c = 0$ and $c = \infty$ with the bounds obtained from (15) and (24), represented as the solid line in this Figure, shows that even these results obtained using only $c = 0$ and $c = \infty$ can produce a relatively small bounding region in the complex plane and that the convex hull is tangent to this region at several points.

7 Algorithm summary

Let us now summarize the algorithm for computing the bounds, *i.e.*, the set B in the complex plane that necessarily contains the desired point y_μ. Given $\kappa_1, \kappa_2, \mu_1$ and μ_2 with positive imaginary parts set

$$\begin{aligned} \theta_U &= \min\{\arg(\kappa_1), \arg(\kappa_2), \arg(\mu_1), \arg(\mu_2)\}, \\ \theta_L &= -\pi + \max\{\arg(\kappa_1), \arg(\kappa_2), \arg(\mu_1), \arg(\mu_2)\}, \end{aligned} \tag{1}$$

where the arguments are to be given in the range from 0 to π, yielding a value θ_U between 0 and π and a value of θ_L between $-\pi$ and 0. Equations (15) and (24) show that for θ continually increasing from θ_L to θ_U, we may plot the curves in the complex Y_μ-plane determined by

$$\begin{aligned} z^-(\theta) &= \frac{\mu_i(8+9c_1)}{6(2+c_1)} + \frac{5(\kappa_j - c_1\mu_i)}{3(2+c_1)^2} \quad \text{and} \\ z^+(\theta) &= \left[\frac{6(2+c_2)}{\mu_k(8+9c_2)} + \frac{60c_2}{(8+9c_2)^2}\left(\frac{c_2}{\kappa_\ell} - \frac{1}{\mu_k}\right)\right]^{-1}, \end{aligned} \tag{2}$$

where, from (10) and (25), the scaling constants satisfy

$$c_1 = \frac{\mathrm{Im}[\kappa_j e^{-i\theta}]}{\mathrm{Im}[\mu_i e^{-i\theta}]} \quad \text{and} \quad c_2 = \frac{\mathrm{Im}[e^{i\theta}/\mu_k]}{\mathrm{Im}[e^{i\theta}/\kappa_\ell]}, \tag{3}$$

and, from (8) and (9), the determining values of the moduli for each angle θ in z^- are

$$\begin{aligned} \mu_i &= \mu_1 \quad \text{if} \quad \mathrm{Im}[(\mu_1 - \mu_2)e^{-i\theta}] \le 0 \\ &= \mu_2 \quad \text{otherwise}, \\ \kappa_j &= \kappa_1 \quad \text{if} \quad \mathrm{Im}[(\kappa_1 - \kappa_2)e^{-i\theta}] \le 0 \\ &= \kappa_2 \quad \text{otherwise}, \end{aligned} \tag{4}$$

while, from (26) and (27), we find for z^+

$$\begin{aligned} \mu_k &= \mu_1 \quad \text{if} \quad \mathrm{Im}[(1/\mu_1 - 1/\mu_2)e^{i\theta}] \ge 0 \\ &= \mu_2 \quad \text{otherwise} \\ \kappa_\ell &= \kappa_1 \quad \text{if} \quad \mathrm{Im}[(1/\kappa_1 - 1/\kappa_2)e^{i\theta}] \ge 0 \\ &= \kappa_2 \quad \text{otherwise}. \end{aligned} \tag{5}$$

Some care in implementation is required if $c_1 \to \infty$ [which happens if one of the shear moduli determines either of the limiting angles in (1)] and/or if $c_2 \to \infty$ [which happens if one of the bulk moduli determines either of the limiting angles, θ_L or θ_U]. At least one of these two cases always obtains. The limiting cases for infinite c values are nevertheless handled quite easily, since the corresponding values of z^- and z^+ are always finite.

Any breaks in the curve $z^-(\theta)$ for $\theta_L \le \theta \le \theta_U$ are joined by straight line segments. (Such breaks are due to changes in the value of μ_i or κ_j. The straight line segment continues the curve at a fixed value of the tangent until the next point at which the tangent may change.) Any breaks in the curve $z^+(\theta)$ for $\theta_L \le \theta \le \theta_U$ are joined by circular arcs which — when extended — pass through the origin. (As for z^-, such breaks are due to changes in the value of μ_k or κ_ℓ. The circular arc passes through the two points defining the break, while the origin is the third point defining the circle.)

The finishing moves for the bounding curves are these: For z^-, two straight lines to infinity are drawn starting at the points $z^-(\theta_L)$ and $z^-(\theta_U)$, both of which are always finite whenever the bulk and shear moduli of the two phases are finite and nonzero. The line issuing from $z^-(\theta_L)$ has slope $m_L = \tan\theta_L$, while the line issuing from $z^-(\theta_U)$ has slope $m_U = \tan\theta_U$. Formulas for these two straight lines are:

$$\begin{aligned} z^- &= z^-(\theta_U) + se^{i\theta_U}, \\ z^- &= z^-(\theta_L) - se^{i\theta_L}, \end{aligned} \tag{6}$$

as s varies from 0 to ∞. For z^+, two circular arcs to the origin are drawn starting at the points $z^+(\theta_L)$ and $z^+(\theta_U)$, both of which are always finite. The arc issuing from $z^+(\theta_L)$ is tangent at the origin to the ray with slope $m_L = \tan\theta_L$, while the arc issuing from $z^+(\theta_U)$ is tangent at the origin to the ray with slope $m_U = \tan\theta_U$. Formulas for these two circular arcs are:

$$\begin{aligned} z^+ &= [1/z^+(\theta_U) + se^{-i\theta_U}]^{-1}, \\ z^+ &= [1/z^+(\theta_L) - se^{-i\theta_L}]^{-1}, \end{aligned} \tag{7}$$

as s varies from 0 to ∞. The correctness of the negative sign preceding s for the second expression in both (6) and (7) may be verified from the observation that $\arg(z^+) = \theta_L + \pi$ must hold in the limit of large s. The closed convex region contained between the two resulting curves ∂B^- and ∂B^+ is the set B. Parts of the curves extending beyond their two points of intersection may be truncated.

Once the bounding region B in the complex Y_μ-plane has been determined by this algorithm, it is straightforward to obtain the corresponding bounding region in the shear modulus plane from (2).

A general purpose code may now be developed wherein the bounding convex hull can be constructed automatically with the only input being the constituent viscoelastic parameters and the volume fractions of the constitutents.

8 Further examples

To complete our analysis, we will present two more examples to illustrate the use of the method.

The next example we consider is $(\kappa_1, \mu_1) = (1, i\,2/3)$ and $(\kappa_2, \mu_2) = (3/2, i\,4/3)$. This example has not been considered previously. It was constructed to highlight the situation in which the two bulk moduli are purely real while the shear moduli are purely imaginary. The colinear ray structure makes this example very similar to the one of Figures 4 and 5.

Results are particularly easy to describe in this problem. Figures 6 and 7 are found in the following way: Using the convex hull formula (15) or (2) with $i = 1$ and $j = 1$, we find that the inner boundary in Figure 6 is constructed as follows. First note that the numerator of c_1 in (3) vanishes as $\theta \to \theta_U = 0$, so the formula in (2) shows that $z^-(\theta) \to 2\mu_i/3 + 5\kappa_j/12 = 5/12 + i4/9$ in this limit. The straight line generated by the first equation in (6) (corresponding to the $c_1 = 0$ limit) is just a horizontal line to the right with $\mathrm{Im}(Y_\mu) = 4/9$ beginning at the point $5/12 + i4/9$. The straight line generated by the second equation in (6) (corresponding to the $c_1 = \infty$ limit) is a straight line from infinity along the imaginary axis to the point $Y_\mu = i$, since (2) shows that $z^-(\theta) \to 3\mu_i/2 = i$. Then, the remainder of the inner boundary is given in a straightforward way by Eq. (2), although some care is required in evaluating c_1 in (3) as $\theta \to \theta_L$. The outer (remaining) boundary of the convex hull is obtained using (24) or (2) with $k = 2$, $l = 2$. Note that the denominator of c_2 vanishes in (3) as $\theta \to \theta_U$, so the formula in (2) shows that $z^+(\theta) \to [2/3\mu_k + 20/27\kappa_\ell]^{-1}$ in this limit. The circular arc generated by the first equation in (7) (corresponding to the limiting circle for $c_2 = \infty$) is the one that passes through the origin and through the point $Y_\mu = i\,2$, while being tangent to the line $\mathrm{Im}(Y_\mu) = 0$ (*i.e.*, the real axis). The part of this circle that contributes to the convex hull boundary is the arc from the origin to the point $[40/81 + 1/2i]^{-1} \simeq 1 + i$. The circular arc generated by the second equation in (7) (corresponding to the limiting boundary for $c = 0$) is the extension of the straight line connecting $Y_\mu = i\,4/9$ and $Y_\mu = i\,2/3$, or just the imaginary axis. Again all the points $z^+(\theta)$ in between are obtained in a straightforward way from (2), although some care must be taken as $\theta \to \theta_U$ since $c_2 \to \infty$ in this limit. We truncate the bounding curves at the two points where the inner and outer boundaries cross. Figure 7 is then found by transforming all points on the resulting truncated boundary from the Y_μ-plane to the complex μ-plane for a 50/50 concentration of the two constituents.

This example demonstrates clearly that there is not necessarily a simple relationship between $z^-(\theta_L)$ and $z^+(\theta_L)$ or between $z^-(\theta_U)$ and $z^+(\theta_U)$. In this example, $\theta_L = -\pi/2$, while $z^-(\theta_L)$ and $z^+(\theta_L)$ both lie on the positive imaginary axis, and thus on the same ray from the origin. However, $\theta_U = 0$ while neither $z^-(0)$ nor $z^+(0)$ lies on the real axis, and furthermore these two points also do not lie on the same ray from the origin.

As our final example, we consider a physically motivated situation in which $(\kappa_1, \mu_1) = (2.2, i\,6.28\times10^{-7})$ and $(\kappa_2, \mu_2) = (44.0 + i\,0.176, 37.0)$. This example has been studied previously by Berryman (1980) to illustrate the results obtained from some effective medium theories for a fluid suspension (at low solid concentrations) and a porous solid saturated with fluid (at high solid concentrations). Type-1 is a fluid-like constituent having the bulk modulus of water ($\kappa_2 = 2.2$ GPa) and the purely imaginary shear modulus of a viscous fluid with formula $\mu_2 = i\omega\eta/\rho_2$, where $\eta = 1.00$ cP, $\rho_2 = 1000.0$ kg/m^3, and $\omega = 2\pi \times 10$ Hz. Type-2 material is a solid such as a sandstone or quartz-rich crystalline rock with a small bulk dissipation component. The results are displayed in Figure 8.

Because μ_1 is such a small quantity compared to other values, results in the Y_μ-plane (not shown) are indistinguishable from the case with $\mu_1 \simeq 0$, but the bounds in the μ-plane do distinguish between these two cases. Considering the limiting values of $c \to 0$ and $c \to \infty$, we find that the bounding curves in the Y_μ-plane are just the real axis and the arc of a circle passing through the point $Y_\mu = (3/2)37.0$, through the origin, and essentially tangent to the imaginary axis at the origin. When the result in the Y_μ-plane is transformed to the μ-plane for a 50/50 concentration of the two constituents, the result is seen in Figure 8. Note that the axes in Figure 8 are plotted on very different scales. We find that the third curve (on the right hand side) of Figure 8 is computed using the convex hull formula (16) as c varies between $c = 0.05946$ and $c = 1.1892$ with $i = 2$ and $j = 2$.

Judging by the observed locations of the Hashin-Shtrikman-Walpole points, the results for this example seem to reflect the fact demonstrated in Section 5 that the extreme Hashin-Shtrikman-Walpole points become true bounds in the limit when all the moduli are real.

As a point of further interest, we have plotted the effective medium result (Berryman, 1980) of the coherent potential approximation (CPA) as the solid square shown in Figure 8. As expected because of the realizability of this theory (Milton 1985; Avellaneda 1987), this point does lie within the rigorous bounds in the complex μ-plane.

9 Discussion

In this paper, we have shown how to derive generalized Hashin-Shtrikman-type variational bounds for the shear modulus of two-component viscoelastic composites in three dimensions. The main result of the paper for applications is summarized in equations (3)-(5). This result was obtained by first developing the general Hashin-Shtrikman variational method for bounds on viscoelastic constants. The results were then specialized to bounds on the shear modulus and a general result was obtained showing that these bounds take the form of circles in the complex plane. One class of suitable restrictions [see (44)] was then placed on the parameters determining the bounds. This choice was subsequently shown to be sufficiently restrictive so that these results reduce precisely to the Hashin-Shtrikman-Walpole bounds when the constituent moduli are all real. The circular bounding regions may be characterized by the fact that they must contain four points determined by the viscoelastic constants (bulk and shear moduli) of the two components of the composite, as well as a point related by the Y_μ-transform to the effective viscoelastic shear modulus. The main results (3)-(5) show that all such bounding circles can be transformed to the Y_μ-plane, so that the intersection of an infinite set of these circular regions may then be used to construct the convex hull of the final bounding region. An analytical means of obtaining the convex hull was derived in Section 6.1, and the resulting general and quite compact algorithm is summarized in (1)-(7).

Results derived are optimal for the Hashin-Shtrikman-type variational principle within the restricted parametrization defined by (44). Some room for improvement remains in the possibility of removing these restrictions and exploring the full six parameter space of constraints. Therefore, we believe the present paper is an intermediate step towards optimal, microgeometry independent bounds on the viscoelastic shear modulus.

The Hashin-Shtrikman variational method is not the only approach that could have been applied to bounding the shear modulus for viscoelastic composites in three dimensions. The translation method could also be used. However, it is not clear which class of "translations" would give the best bounds, or even which would give the simplest useful bounds. Being more complicated than what we have already done, we have left the development of the translation method for the problem of viscoelastic shear moduli to future work.

The present paper has been limited to shear modulus bounds for three dimensional viscoelastic composites. More restrictive results are known for two dimensions and these bounds will be presented in the next paper in this series. Comparisons to experimental data and further comparisons to alternative theoretical means of estimating viscoelastic constants will appear elsewhere.

Acknowledgments

We thank Paul Wessel for the use of his computer graphics software. We thank Leonid Gibiansky for many helpful discussions, especially concerning potential improvements to the theory in two-dimensions. The work of GWM was supported by the National Science Foundation through grants DMS-9501025 and DMS-9402763. The work of JGB was performed under the auspices of the U. S. Department of Energy by the Lawrence Livermore National Laboratory under contract No. W-7405-ENG-48 and supported specifically by the Geosciences Research Program of the DOE Office of Energy Research within the Office of Basic Energy Sciences, Division of Engineering and Geosciences. Some work performed by JGB while visiting the Geophysics Department at Stanford University with partial support from the Stanford Exploration Project and its sponsors. All support of this work is hereby gratefully acknowledged.

Appendix – Reference Tensor

To understand how to proceed towards definite results from the Hashin-Shtrikman-type bounding relation (28), we need to analyze the expression $\tilde{\Gamma}\mathbf{D}_0\tilde{\Gamma}$ appearing there. To do so, we express the matrix in terms of four orthogonal projection operators $\Gamma_{1,h}$, $\Gamma_{1,s}$, $\Gamma_{2,h}$, $\Gamma_{2,s}$ projecting respectively onto ε_h, ε_s, σ_h, σ_s. [See Milton & Kohn (1988) for more details concerning these definitions and for explicit expressions in Fourier space.] Recalling the definition of $\mathbf{D}_0$ in (8), we find

$$\tilde{\Gamma}\mathbf{D}_0\tilde{\Gamma} = \begin{pmatrix} a_{11,h}\Gamma_{2,h} + a_{11,s}\Gamma_{2,s} & a_{12}\Gamma_{2,h}\Lambda_h\Gamma_{1,h} \\ a_{12}\Gamma_{1,h}\Lambda_h\Gamma_{2,h} & a_{22,h}\Gamma_{1,h} + a_{22,s}\Gamma_{1,s} \end{pmatrix}, \tag{1}$$

where the constants appearing in (1) are given in terms of the dimension d and constants from the definition (8) of $\mathbf{D}_0$ by

$$a_{11,h} = \frac{(d-1)\alpha_{11}}{d^2} + \frac{\beta_{11}}{2d}, \tag{2}$$

$$a_{11,s} = \frac{\beta_{11}}{2}, \qquad a_{12} = \alpha_{12} - \beta_{12}, \qquad a_{22,s} = 2\beta_{22}, \tag{3}$$

and

$$a_{22,h} = \alpha_{22} + \frac{2(d-1)\beta_{22}}{d}. \tag{4}$$

[Note that the matrix element corresponding to (4) was printed incorrectly in Eq. (4.23) of Part I, and that another related typographical error occurred in (4.25) of Part I.]

The inverse of (1) may be written in the same general form as

$$\tilde{\Gamma}_{D_0} = \begin{pmatrix} b_{11,h}\Gamma_{2,h} + b_{11,s}\Gamma_{2,s} & b_{12}\Gamma_{2,h}\Lambda_h\Gamma_{1,h} \\ b_{12}\Gamma_{1,h}\Lambda_h\Gamma_{2,h} & b_{22,h}\Gamma_{1,h} + b_{22,s}\Gamma_{1,s} \end{pmatrix}, \tag{5}$$

where the constants appearing in (5) are given by

$$b_{11,s} = \frac{1}{a_{11,s}}, \qquad b_{22,s} = \frac{1}{a_{22,s}}, \tag{6}$$

$$b_{12} = \frac{a_{12}d^2}{a_{12}^2(d-1) - d^2 a_{22,h}a_{11,h}}, \tag{7}$$

$$b_{11,h} = -\frac{a_{22,h}d^2}{a_{12}^2(d-1) - d^2 a_{22,h}a_{11,h}}, \tag{8}$$

and

$$b_{22,h} = -\frac{a_{11,h}d^2}{a_{12}^2(d-1) - d^2 a_{22,h}a_{11,h}}. \tag{9}$$

To obtain these results, we have used the identities [see the Appendix of Milton & Kohn (1988) for more details]

$$\Gamma_{2,h}\Lambda_h\Gamma_{1,h}\Lambda_h\Gamma_{2,h} = \frac{1}{d}\Gamma_{2,h}\Lambda_h\Gamma_{2,h} = \frac{d-1}{d^2}\Gamma_{2,h}, \tag{10}$$

and

$$\Gamma_{1,h}\Lambda_h\Gamma_{2,h}\Lambda_h\Gamma_{1,h} = \frac{d-1}{d}\Gamma_{1,h}\Lambda_h\Gamma_{1,h} = \frac{d-1}{d^2}\Gamma_{1,h}. \tag{11}$$

For the shear modulus bounds, we may take the operator $\mathbf{M}$ to have the symmetrical outer product form

$$\mathbf{M} = \begin{pmatrix} w_1\Lambda_s \\ w_2\Lambda_s \end{pmatrix} \begin{pmatrix} w_1\Lambda_s & w_2\Lambda_s \end{pmatrix}, \tag{12}$$

where w_1,w_2 are arbitrary scalars. Then, we find the trace

$$\mathrm{Tr}\{\mathbf{M}\tilde{\Gamma}_{D_0}\} = \\ \begin{pmatrix} w_1 & w_2 \end{pmatrix} \begin{pmatrix} \frac{1}{d}b_{11,h} + \frac{(d-2)(d+1)}{2}b_{11,s} & -\frac{d-1}{d^2}b_{12} \\ -\frac{d-1}{d^2}b_{12} & \frac{d-1}{d}b_{22,h} + (d-1)b_{22,s} \end{pmatrix} \begin{pmatrix} w_1 \\ w_2 \end{pmatrix}, \tag{13}$$

obtained using (5) and (29). For future reference, we will define the 2×2 matrix appearing in (13) to be the inverse of a matrix $\mathbf{A}_d$, where d is the dimension appearing explicitly in the formula. Then, for $d = 3$, we have

$$\mathbf{A}_3^{-1} = \begin{pmatrix} \frac{1}{3}b_{11,h} + 2b_{11,s} & -\frac{2}{9}b_{12} \\ -\frac{2}{9}b_{12} & \frac{2}{3}b_{22,h} + 2b_{22,s} \end{pmatrix}. \tag{14}$$

We note that many of the formulas in this Appendix simplify greatly if the reference tensor is chosen so that $\alpha_{12} = \beta_{12}$. Then, both $a_{12} = 0$ and $b_{12} = 0$, showing that the off-diagonal terms in (1), (5), and (14) all vanish. The reason for this simplification is that the off-diagonal tensor blocks of the reference tensor itself are in this case of the form $\alpha_{12}\mathbf{I}$, which then are easily shown to contribute a null-Lagrangian to the pertinent energy functional and therefore cannot contribute to the final results. We take advantage of this simplification in the present paper even though it may not lead to the best results that can be obtained from the general methods presented.

References

Avellaneda, M. 1987 Iterated homogenization, differential effective medium theory and applications, *Commun. Pure Appl. Math.* **40**, 527–554.

1216–1228.

Bergman, D. J. 1980 Exactly solvable microscopic geometries and rigorous bounds for the complex dielectric constant of a two-component composite material. *Phys. Rev. Lett.* **44**, 1285–1287.

Bergman, D. J. 1982 Rigorous bounds for the complex dielectric constant of a two component composite. *Ann. Phys.* **138**, 78–114.

Berryman, J. G. 1980 Long-wavelength propagation in composite elastic media II. Ellipsoidal inclusions. *J. Acoust. Soc. Am.* **68**, 1820–1831.

Berryman, J. G. 1985 Measurement of spatial correlation functions using image processing techniques, *J. Appl. Phys.* **57**, 2374–2384.

Brinson, L. C. & Lin, W. S. 1997 Comparison of micromechanics methods for effective properties of multiphase viscoelastic composites. *Mech. Materials*, submitted.

Cherkaev, A. V., & Gibiansky, L. V. 1994 Variational principles for complex conductivity, viscoelasticity, and similar problems in media with complex moduli. *J. Math. Phys.* **35**, 1–19.

Christensen, R. M. 1969 Viscoelastic properties of heterogeneous media. *J. Mech. Phys. Solids* **17**, 23–41.

Fannjiang, A., & Papanicolaou, G. 1994 Convection enhanced diffusion in periodic flows. *SIAM J. Appl. Math.* **54**, 333–408.

Francfort, G. A., & Murat, F. 1986 Homogenization and optimal bounds in linear elasticity. *Archive Rational Mech. Anal.* **94**, 307–334.

Gibiansky, L. V., & Lakes, R. 1993 Bounds on the complex bulk modulus of a two-phase viscoelastic composite with arbitrary volume fractions of the components. *Mech. Materials* **16**, 317–331.

Gibiansky, L. V., & Lakes, R. 1997 Bounds on the complex bulk and shear moduli of a two-dimensional two-phase viscoelastic composite. *Mech. Materials*, in press.

Gibiansky, L. V., Lakes, R., & Milton, G. W. 1993 Viscoelastic composites with extremal properties. In *Structural Optimization 93*, Vol. I, edited by J. Herskovits, Proceedings of the World Congress on Optimal Dsign of Structural Systems, Rio de Janeiro, Brazil, August 2–6, 1993, pp. 369–376.

Gibiansky, L. V., & Milton, G. W. 1993 On the effective viscoelastic moduli of two-phase media. I. Rigorous bounds on the complex bulk modulus. *Proc. R. Soc. London A* **440**, 163–188.

Gibiansky, L. V., & Milton, G. W. 1997 Shear modulus bounds for planar viscoelastic two-phase composites, *unpublished manuscript.*

Gibiansky, L. V., & Torquato, S. 1997 New method to generate three-point bounds on effective properties of composites: Application to viscoelasticity. *J. Mech. Phys. Solids*, submitted.

Hashin, Z. 1965 Viscoelastic behaviour of heterogeneous media. *ASME J. Appl. Mech.* **32**, 630–636.

Hashin, Z. 1970 Complex moduli of viscoelastic composites. I. General theory and application to particulate composites. *Int. J. Solids Structures* **6**, 539–552. II. Fiber reinforced materials. *Int. J. Solids Structures* **6**, 797–807.

Hashin, Z. 1983 Analysis of composite materials — A survey. *J. Appl. Mech.* **50**, 481–505.

Hashin, Z., & Shtrikman, S. 1963 A variational approach to the theory of the elastic behaviour of multiphase materials. *J. Mech. Phys. Solids* **11**, 127–140.

Li, J., & Weng, G. J. 1994 Strain-rate sensitivity, relaxation behavior, and complex moduli of a class of isotropic viscoelastic composites. *ASME J. Engineering Materials Techn.* **116**, 495–504.

Li, J. & Weng, G. J. 1997 Influence of inclusion microgeometry on some thermomechanical properties of isotropic polymer-matrix composites. *ASME J. Engineering Materials Techn.*, submitted.

Lurie, K. A., & Cherkaev, A. V. 1984 The problem of formation of an optimal isotropic multicomponent composite. *Report N. 895, Phys.-Tech. Inst. Acad. Sci.*, in Russian.

Lurie, K. A., & Cherkaev, A. V. 1986 The effective characteristics of composite materials and optimal design of constructions. *Adv. Mech. (Poland)* **9**, 3–81.

Milton, G. W. 1980 Bounds on the complex dielectric constant of a composite material. *Appl. Phys. Lett.* **37**, 300–302.

Milton, G. W. 1981 Bounds on the complex permittivity of a two-component composite material. *J. Appl. Phys.* **52**, 5286–5293.

Milton, G. W. 1985 The coherent potential approximation is a realizable effective medium theory. *Commun. Math. Phys.* **99**, 463–500.

Milton, G. W. 1986 Modelling the properties of composites by laminates. In *Homogenization and Effective Moduli of Materials and Media*, J. Ericksen, D. Kinderlehrer, R. Kohn, and J. L. Lions (eds.), Springer-Verlag, New York, pp. 150–174.

Milton, G. W. 1990 On characterizing the set of possible effective tensors of composites: The variational method and the translation method. *Commun. Pure Appl. Math.* **43**, 63–125.

Milton, G. W., & Kohn, R. V. 1988 Variational bounds on the effective moduli of anisotropic composites, *J. Mech. Phys. Solids*, *36*, 597–629.

Milton, G. W., & Phan-Thien, N. 1982 New bounds on effective elastic moduli of two-component materials. *Proc. R. Soc. London* **A 380**, 305–331.

Murat, F., & Tartar, L. 1985 Calcul des variations et homogénéisation. In *Les méthodes d'homogénéisation: théorie et applications en physique, Coll. de la Dir. des Études et Recherches d'Electr. de France, Eyrolles, Paris*, pp. 319–370.

Norris, A. N. 1985 A differential scheme for the effective moduli of composites. *Mech. Mater.* **4**, 1–16.

Roscoe, R. 1969 Bounds for real and imaginary parts of the dynamic moduli of composite viscoelastic systems. *J. Mech. Phys. Solids* **17**, 17–22.

Roscoe, R. 1972 Improved bounds for real and imaginary parts of complex moduli of isotropic viscoelastic composites. *J. Mech. Phys. Solids* **20**, 91–99.

Torquato, S. 1991 Random heterogeneous media: Microstructure and improved bounds on effective properties. *Appl. Mech. Rev.* **44**, 37–76.

Walpole, L. J. 1966 On bounds for the overall elastic moduli of inhomogeneous systems. I. *J. Mech. Phys. Solids* **14**, 151–162.

Zhikov, V. V. 1991 Estimates for the homogenized matrix and the homogenized tensor. *Uspekhi Mat. Nauk.* **46**, 49–109. (English translation: *Russ. Math. Surv.* **46**, 65–136.)

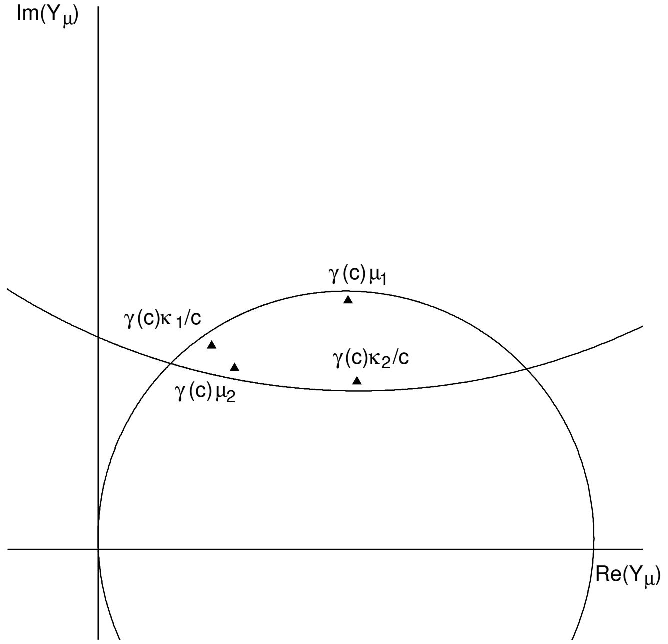

Figure 1: Schematic showing arcs of two circular bounding regions in the complex Y_μ-plane both of which contain the desired y_μ point. Triangles are the four points in Eq. (1.3) for a particular value of the scaling parameter c. By examining all values of c in its range $0 \leq c \leq \infty$, the intersection set of all such regions determines the final bounding set for y_μ.

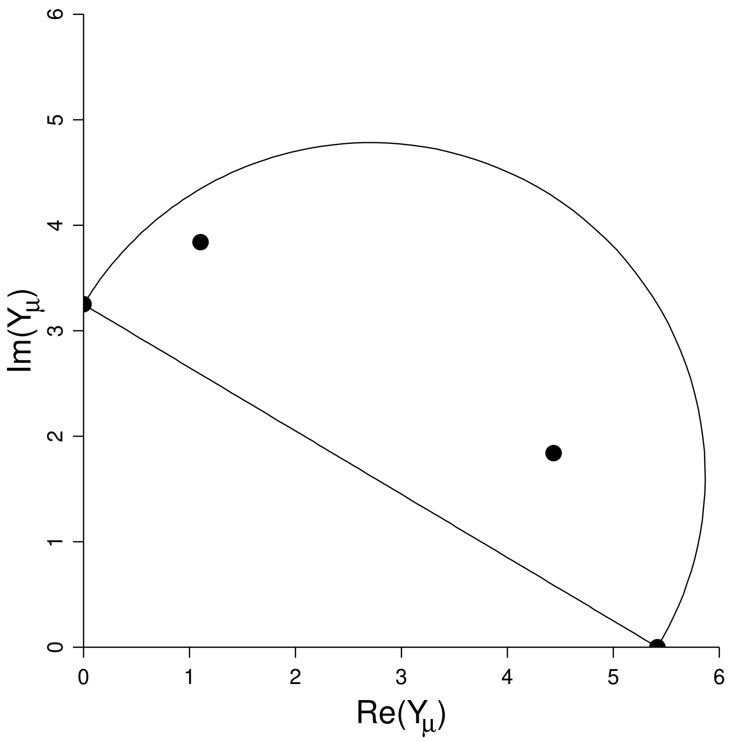

Figure 2: Bounding region in the Y_μ-plane when $(\kappa_1, \mu_1) = (i\,6.0, i\,3.0)$ and $(\kappa_2, \mu_2) = (10.0, 5.0)$. Dots are the four Hashin-Shtrikman-Walpole points.

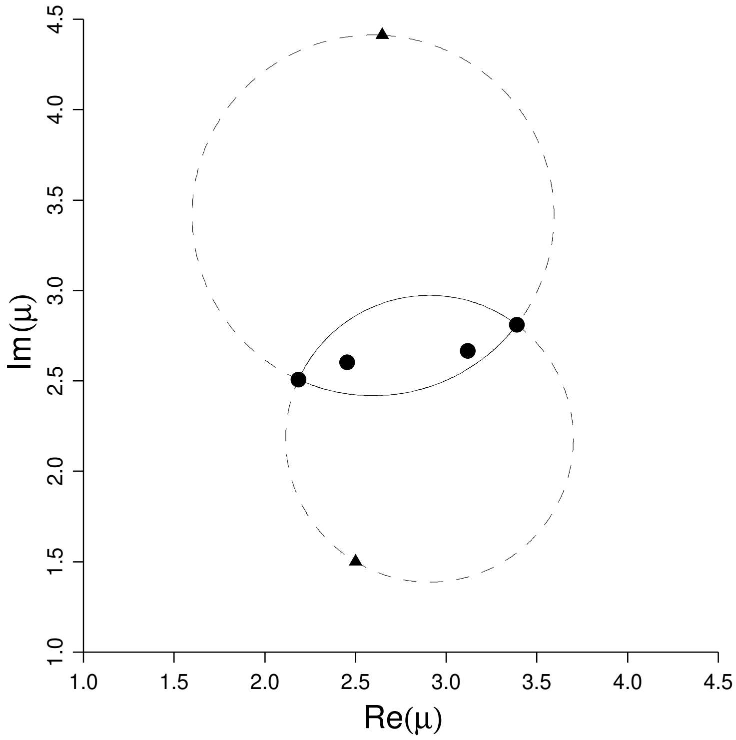

Figure 3: Bounding region in the μ-plane when $(\kappa_1, \mu_1) = (i6.0, i3.0)$ and $(\kappa_2, \mu_2) = (10.0, 5.0)$. Dots are the four Hashin-Shtrikman-Walpole points. Triangles are the Reuss and Voigt points (corresponding, respectively, to the origin and to infinity in the Y_μ-plane). The circles illustrate the method of construction of the bounds in this particularly simple case.

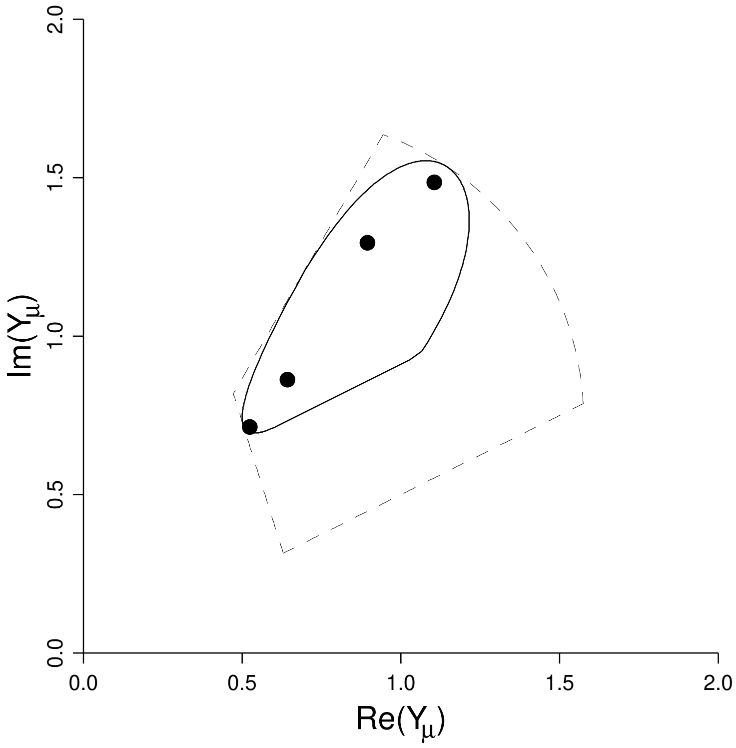

Figure 4: Bounding region in the Y_μ-plane when $(\kappa_1, \mu_1) = (0.667 + i\,0.333, 0.5 + i\,0.866)$ and $(\kappa_2, \mu_2) = (1.667 + i\,0.833, 1.0 + i\,1.732)$. Solid lines form the boundary of the convex hull. Dashed lines are the boundary for the intersection of the bounding sets for $c = 1$. Dots are the four Hashin-Shtrikman-Walpole points.

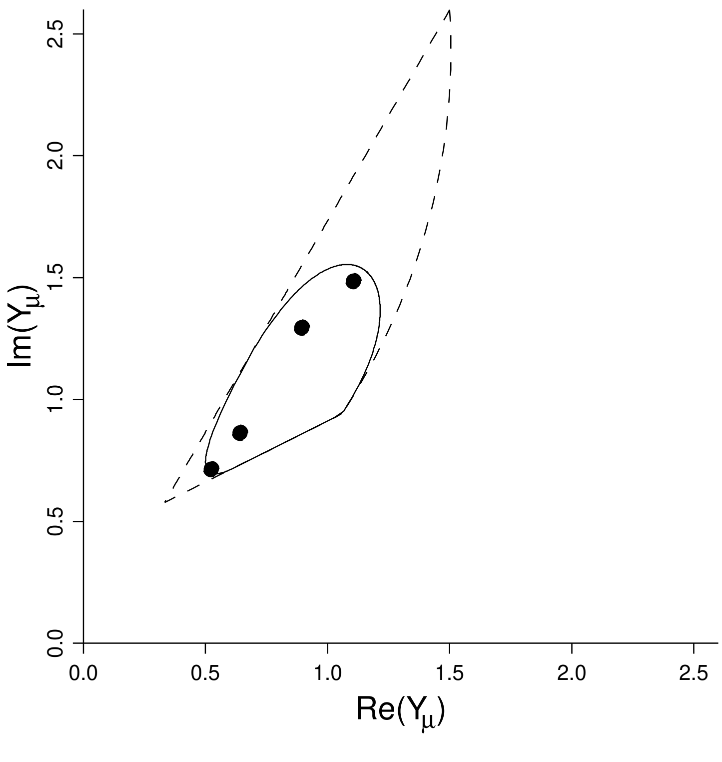

Figure 5: Bounding region in the Y_μ-plane when $(\kappa_1, \mu_1) = (0.667 + i\,0.333, 0.5 + i\,0.866)$ and $(\kappa_2, \mu_2) = (1.667 + i\,0.833, 1.0 + i\,1.732)$. Solid lines form the boundary of the convex hull. Dashed lines are the boundary for the intersection of the bounding sets for $c = 0$ and $c = \infty$. Dots are the four Hashin-Shtrikman-Walpole points.

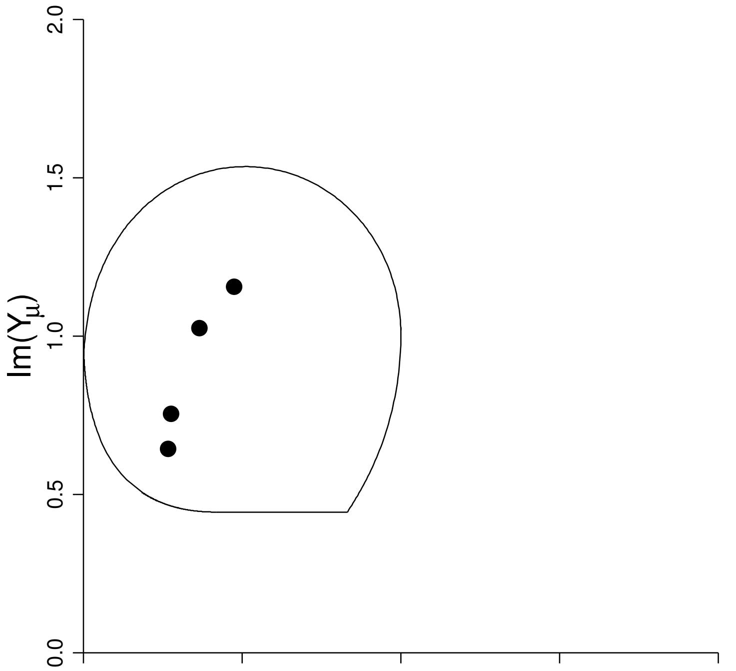

Figure 6: Bounding region in the Y_μ-plane when $(\kappa_1, \mu_1) = (1.0, i\,0.6667)$ and $(\kappa_2, \mu_2) = (1.5, i\,1.333)$. Dots are the four Hashin-Shtrikman-Walpole points.

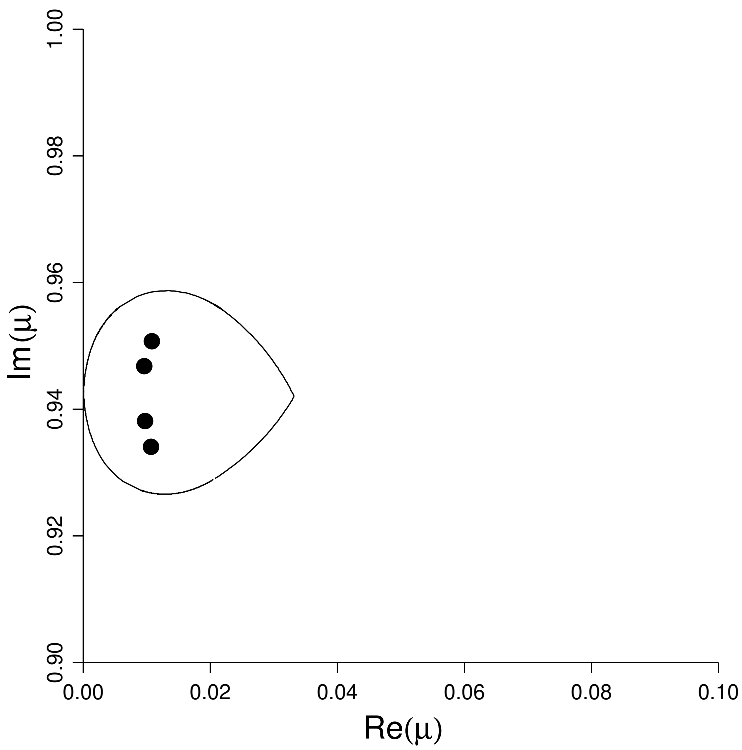

Figure 7: Bounding region in the μ-plane when $(\kappa_1, \mu_1) = (1.0, i\,0.6667)$ and $(\kappa_2, \mu_2) = (1.5, i\,1.333)$. Dots are the four Hashin-Shtrikman-Walpole points.

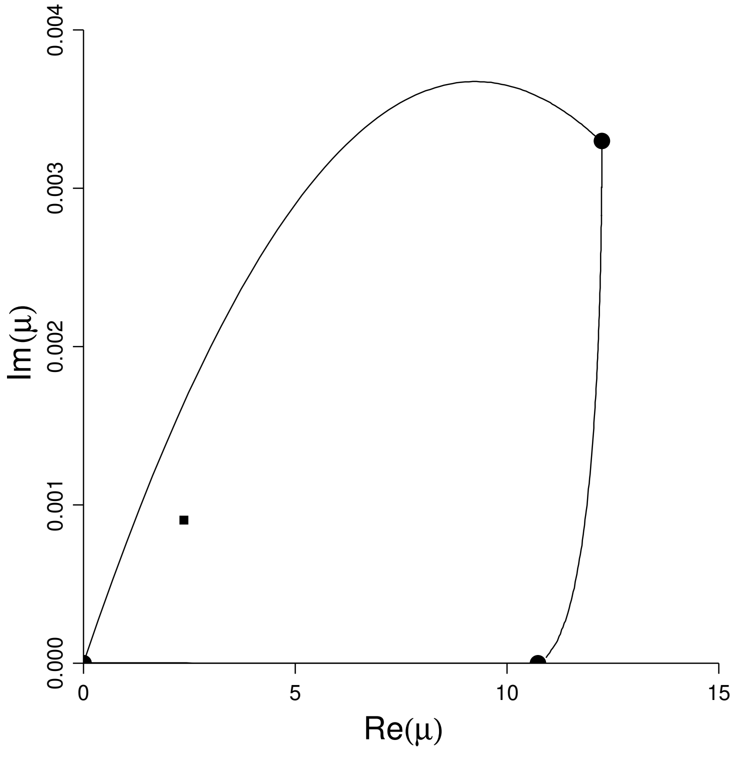

Figure 8: Bounding region in the μ-plane when $(\kappa_1, \mu_1) = (2.2, i\,6.28 \times 10^{-7})$ and $(\kappa_2, \mu_2) = (44.0 + i\,0.176, 37.0)$. Dots are the four Hashin-Shtrikman-Walpole points, two of which are indistinguishable (near the origin) on this plot. The square shows the location of the coherent potential approximation (CPA) effective medium result.